

Some considerations on the restoration of Galilei invariance in the nuclear many-body problem

Part II: Electromagnetic properties of simple bound states

K.W. Schmid^a

Institut für Theoretische Physik der Universität Tübingen, Auf der Morgenstelle 14, D-72076 Tübingen, FRG

Received: 21 February 2001 / Revised version: 18 December 2001

Communicated by D. Schwalm

Abstract. The effects of the restoration of Galilei invariance in the nuclear many-body problem on the electromagnetic properties of simple bound states are investigated. For this purpose the form factors for elastic electron scattering from the oscillator ground states of ${}^4\text{He}$, ${}^{16}\text{O}$ and ${}^{40}\text{Ca}$ as well as those for elastic and inelastic electron scattering between various one-hole states with respect to these reference configurations are computed with and without projection into the center-of-momentum rest frame. It is demonstrated that, in some cases, the full restoration of Galilei invariance produces results which are considerably different from those obtained with the usual approximate way to treat the center-of-mass motion. The same holds for the mathematical Coulomb sum rules and their first and second moments obtained for the above-mentioned nuclei.

PACS. 21.60.-n Nuclear-structure models and methods

1 Introduction

This is the second paper in a series of six articles. In the first one [1] it was shown how Galilei invariance can be restored in the nuclear many-body problem with the help of projection techniques. This paper was devoted to the development of the mathematical tools needed to project simple bound oscillator configurations into their center-of-momentum (COM) rest frame and to calculate the matrix elements of arbitrary operators between such projected states. Furthermore, as a first application, in this paper the spectral functions and spectroscopic factors of the uncorrelated oscillator ground states of the three doubly even nuclei ${}^4\text{He}$, ${}^{16}\text{O}$ and ${}^{40}\text{Ca}$ were investigated with and without projection into the COM rest frame. In complete agreement with earlier studies of the spectroscopic factors [2], it turned out that the simple picture of an uncorrelated system is modified quite drastically if Galilei invariance is respected. For the deep-lying hole states one obtained a considerable depletion of the occupation due to the removal of the spurious admixtures resulting from the COM motion. This was compensated by an “over-occupation” of the (non-spurious) holes within the last occupied shell so that the sum rules for the total hole strengths are conserved. Similar effects were seen for the particle spectroscopic factors.

In the present article, we shall consider the electromagnetic properties of simple bound configurations as they are seen in elastic electron scattering from the oscillator ground states of the above-mentioned three doubly even nuclei as well as in elastic and inelastic electron scattering between the corresponding various one-hole configurations. If initial and final states are both “non-spurious” oscillator configurations (*i.e.*, the COM is in its $0s$ oscillator ground state) then the restoration of Galilei invariance is trivial: we simply have to modify the normal description of the corresponding form factors by the so-called “Tassie-Barker factor” [3]. In case that target and/or final state contain spurious admixtures due to the COM motion, however, this prescription is not sufficient. So, *e.g.*, considerable effects of the full restoration of Galilei invariance on top of the Tassie-Barker correction are seen already in the elastic scattering from doubly even one-determinant ground states, if for the latter not simple oscillator configurations but Woods-Saxon or Skyrme-Hartree-Fock wave functions are used [4,5]. Such “general determinants”, however, will not be considered in the present paper. Instead, we restrict ourselves as already in ref. [1] entirely to simple oscillator configurations. This has the advantage that all the relevant matrix elements can be computed analytically. Furthermore this restriction is a “conservative approach”: the effects discussed in the following are a kind of “lower limit” of what has to be expected in more realistic calculations. Any generalisation of the wave functions will only increase the effects.

^a e-mail: karl-wilhelm.schmid@uni-tuebingen.de

Obviously, since the oscillator ground states of the above-mentioned three doubly even nuclei as well as the corresponding one-hole configurations with the hole out of the last occupied shell are “non-spurious”, effects on top of the Tassie-Barker correction can only be expected for the scattering between various one-hole configurations with at least one of the hole states not from the last occupied shell. It will be these processes which are studied in detail in the following. For completeness, however, the results for scattering between non-spurious states will be presented in an appendix, too.

Besides the charge and current form factors in the present article also the effects of the restoration of Galilei invariance on the (mathematical) Coulomb sum rule and their first and second moments will be investigated.

2 Electromagnetic properties

In subsect. 2.1 we shall derive the matrix elements of general one-body operators with and without projection into the COM rest frame. Subsection 2.2 will then present the electromagnetic form factors between various simple oscillator configurations. Since we are interested in the differences of the projected with respect to the “normal” results we do not restrict ourselves to those transitions from the ground-state configuration of the target to itself or to excited states but shall consider the transitions between the various excited configurations, too. For completeness, the results for the transitions not discussed in this section will be given in the appendix. Subsection 2.3 then is devoted to the (mathematical) Coulomb sum rule and its first and second moments.

2.1 General one-body operators

In the momentum space representation the one-body operators used in the following can be written as

$$\hat{O} \equiv \sum_{12} \int d^3\vec{k}_1 o_{12}(\vec{\kappa}_1, \vec{\lambda}) c_{\vec{k}_1 1}^\dagger c_{\vec{k}_1 - \vec{q} 2}, \quad (2.1)$$

where $1 \equiv \sigma_1, \tau_1$, $2 \equiv \sigma_2, \tau_2$, $\vec{\kappa}_1 \equiv b\vec{k}_1$, $\vec{\lambda} \equiv b\vec{q}$ and \vec{q} is the total momentum transfer to the considered system.

One example for such one-body operators is the kinetic energy. Here the momentum transfer $\vec{q} = 0$ and

$$t_{12}(\vec{\kappa}_1) \equiv o_{12}(\vec{\kappa}_1, 0) = \Delta_{12} \frac{(\hbar c)^2}{2Mc^2} \frac{1}{b^2} \kappa_1^2 = \Delta_{12} \frac{\hbar\omega}{2} \kappa_1^2. \quad (2.2)$$

This operator will be treated in more detail in the next article of the present series of papers. The example studied in the present article are the charge density and current operators. Details on these operators can be found, *e.g.*, in ref. [6]. They are obtained as usual by a Foldy-Wouthuysen reduction [7] (up to order one over the square of the nucleon mass) of the Dirac equation for the nucleon interacting with the electromagnetic field of the passing electron. Note that this derivation is based on the assumption that

the electromagnetic form factors of the nucleons can be replaced by the free ones even in the nuclear medium. We shall restrict ourselves here to one-body currents only. Since we shall be using phenomenological strong interactions throughout the present series of papers, the inclusion of meson exchange currents would not be consistent, anyhow.

For the charge density operator one obtains the form (2.1) with

$$\rho_{12}(\vec{\lambda}) \equiv o_{12}(\vec{\kappa}_1, \vec{\lambda}) = \Delta_{12} f_{\tau_1}(Q^2), \quad (2.3)$$

where the nucleon charge form factors f_τ are given by

$$f_\tau(Q^2) \equiv G_E^\tau(Q^2) - \frac{Q^2}{8M^2} \frac{G_E^\tau(Q^2) + \frac{Q^2}{4M^2} G_M^\tau(Q^2)}{1 + \frac{Q^2}{4M^2}} \quad (2.4)$$

with the Sachs form factors usually parametrized in the well-known dipole form (see, *e.g.*, Preston and Bhaduri [8])

$$\begin{aligned} G_E^p(Q^2) &\equiv \left[1 + \frac{Q^2}{(843 \text{ MeV})^2} \right]^{-2}, \\ G_M^\tau(Q^2) &\equiv \mu_\tau G_E^p(Q^2), \quad \text{with } \begin{cases} \mu_p = +2.793 \\ \mu_n = -1.913 \end{cases}, \\ G_E^n(Q^2) &\equiv -\mu_n \frac{Q^2}{4M^2} \frac{1}{1 + 5.6 \frac{Q^2}{4M^2}} G_E^p(Q^2). \end{aligned} \quad (2.5)$$

They depend on the (negative) square of the 4-momentum transfer

$$Q^2 \equiv (\hbar c\vec{q})^2 - (\Delta E)^2, \quad (2.6)$$

with ΔE being the energy transfer to the system. Note that because of (2.6), the charge density operator (2.3) depends on the 3-momentum transfer as well as the energy transfer. For simplicity we have not introduced ΔE explicitly as argument on the left side of (2.3). The same holds for the convection (2.7) and spin current (2.9) operators defined below. Furthermore, (2.3), (2.7) and (2.9) are all given in units of the elementary charge e .

The corresponding current operator can be split into two parts. The first is the convection current

$$\left[\vec{j}_{12}^{\text{cc}} \right]_s(\vec{\kappa}_1, \vec{\lambda}) \equiv o_{12}(\vec{\kappa}_1, \vec{\lambda}) = \Delta_{12} f_{\tau_1}^{\text{cc}}(Q^2) \frac{\hbar c}{Mc^2 b} [\vec{\kappa}_1]_s, \quad (2.7)$$

from which, because of Siegert's theorem only the transverse components, *i.e.*, those perpendicular to \vec{q} , are needed. This is indicated by the subscript s . If as usual the z -axis is chosen in the direction of the momentum transfer, then $s = x, y$ in the Cartesian, or $s = \pm 1$ in the spherical representation. The nucleon form factors for the convection current are given by

$$f_\tau^{\text{cc}}(Q^2) \equiv \frac{G_E^\tau(Q^2) + \frac{Q^2}{4M^2} G_M^\tau(Q^2)}{1 + \frac{Q^2}{4M^2}}. \quad (2.8)$$

The second part is the spin current

$$\begin{aligned} \left[\vec{j}_{12}^{\text{sc}} \right]_s(\vec{\lambda}) &\equiv o_{12}(\vec{\kappa}_1, \vec{\lambda}) = \\ &\delta_{\tau_1 \tau_2} G_M^{\tau_1}(Q^2) \frac{\hbar c}{Mc^2 b} \left\langle \sigma_1 \left| \frac{i}{2} \left[\vec{\sigma} \times \vec{\lambda} \right]_s \right| \sigma_2 \right\rangle, \end{aligned} \quad (2.9)$$

which is already purely transverse. In spherical representation we have (with \vec{q} in \vec{z} -direction)

$$\left\langle \sigma_1 \left| \frac{i}{2} (\vec{\sigma} \times \vec{\lambda}) \right| \sigma_2 \right\rangle = \delta_{\sigma_1 \pm 1/2} \delta_{\sigma_2 \mp 1/2} \frac{\lambda}{\sqrt{2}}. \quad (2.10)$$

Note, that (2.3) and (2.7) conserve the spin projection while the spin current (2.9) induces a spin-flip. In actual measurements convection and spin currents cannot be separated but will contribute simultaneously and do interfere. However, out of pedagogical reasons we shall treat them separately in the present paper.

Because of the momentum transfer, the form (2.1) does not conserve the total linear momentum. To be used in COM-projected calculations it has to be multiplied with the so-called Gartenhaus-Schwartz operator $\exp\{-i\vec{q} \cdot \vec{R}_A\}$ (see, *e.g.*, ref. [6]) which compensates for the transferred momentum. In normal space representation this operator comes from writing the one-body operators (2.3), (2.7) and (2.9) in relative coordinates $\vec{r}_i - \vec{R}_A$ and relative momenta $\hat{p}_i - \hat{P}_A/A$, where \vec{R}_A and \hat{P}_A are the center-of-mass coordinate and the operator of the total linear momentum as defined in eq. (1.2) of ref. [1]. Because of that, obviously, the Galilei-invariant form of a general one-body operator,

$$\hat{O}_A^{\text{inv}} \equiv \hat{O} \exp\{-i\vec{q} \cdot \vec{R}_A\}, \quad (2.11)$$

is A -dependent as indicated by the subscript A .

Note, that this modification is sufficient for the convection current, too. The use of relative momenta induces here only additional terms proportional to \vec{q} , which are longitudinal and hence not needed, and terms proportional to \hat{P}_A which are irrelevant because we project into the COM rest frame.

We start by calculating the expectation value of (2.1) within our reference determinants $|\rangle$. We obtain

$$\begin{aligned} \langle |\hat{O}| \rangle &= \sum_{12} \int d^3 \vec{k}_1 o_{12}(\vec{\kappa}_1, \vec{\lambda}) \langle |c_{\vec{k}_1 1}^\dagger c_{\vec{k}_1 - \vec{q} 2}| \rangle = \sum_1 \frac{1}{\pi \sqrt{\pi}} \\ &\cdot \int d^3 \vec{\kappa}_1 o_{11}(\vec{\kappa}_1, \vec{\lambda}) \exp\{-\kappa_1^2 + \vec{\kappa}_1 \cdot \vec{\lambda} - \lambda^2/2\} y(\vec{\kappa}_1 - \vec{\lambda}, \vec{\kappa}_1) = \\ &\exp\left\{-\frac{1}{4}\lambda^2\right\} \frac{1}{\pi \sqrt{\pi}} \int d^3 \vec{z} \exp\{-z^2\} \\ &\cdot \sum_1 o_{11}(\vec{z} + \vec{\lambda}/2, \vec{\lambda}) y(\vec{z} - \vec{\lambda}/2, \vec{z} + \vec{\lambda}/2) = \exp\left\{-\frac{1}{4}\lambda^2\right\} \\ &\cdot \frac{1}{\pi \sqrt{\pi}} \int d^3 \vec{z} \exp\{-z^2\} \sum_1 o_{11}(\vec{z} + \vec{\lambda}/2, \vec{\lambda}) \\ &\cdot \begin{cases} 1 & \text{for } ^4\text{He} \\ 1 + 2z^2 - \lambda^2/2 & \text{for } ^{16}\text{O} \\ 5/2 + 2z^4 - \lambda^2 z^2 - \lambda^2 + \lambda^4/8 & \text{for } ^{40}\text{Ca} \end{cases}, \quad (2.12) \end{aligned}$$

where we have used eq. (2.25) with $\vec{\kappa}_1 = \vec{z} + \vec{\lambda}/2$ and the functions y out of eq. (2.26) from ref. [1].

For the matrix elements of (2.1) in between two one-hole states one gets in the same way

$$\begin{aligned} \langle |b_{Hh}^\dagger \hat{O} b_{H'h'}| \rangle &= \sum_{12} \int d^3 \vec{k}_1 o_{12}(\vec{\kappa}_1, \vec{\lambda}) \\ &\cdot \langle |b_{Hh}^\dagger c_{\vec{k}_1 1}^\dagger c_{\vec{k}_1 - \vec{q} 2} b_{H'h'}| \rangle = \sum_{12} \frac{1}{\pi \sqrt{\pi}} \int d^3 \vec{\kappa}_1 o_{12}(\vec{\kappa}_1, \vec{\lambda}) \\ &\cdot \exp\{-\kappa_1^2 + \vec{\kappa}_1 \cdot \vec{\lambda} - \lambda^2/2\} \left\{ \Delta_{12} \Delta_{h'h} \delta_{H'H} y(\vec{\kappa}_1 - \vec{\lambda}, \vec{\kappa}_1) \right. \\ &\left. - \Delta_{1h'} \Delta_{2h}(\vec{\kappa}_1 - \vec{\lambda}|H)(H'|\vec{\kappa}_1) \right\} = \exp\left\{-\frac{1}{4}\lambda^2\right\} \frac{1}{\pi \sqrt{\pi}} \\ &\cdot \int d^3 \vec{z} \exp\{-z^2\} \sum_{12} o_{12}(\vec{z} + \vec{\lambda}/2, \vec{\lambda}) \\ &\cdot \left\{ \Delta_{12} \Delta_{h'h} \delta_{H'H} y(\vec{z} - \vec{\lambda}/2, \vec{z} + \vec{\lambda}/2) \right. \\ &\left. - \Delta_{1h'} \Delta_{2h}(\vec{z} - \vec{\lambda}/2|H)(H'|\vec{z} + \vec{\lambda}/2) \right\}, \quad (2.13) \end{aligned}$$

where we have used eqs. (2.23) to (2.25) from ref. [1], again with $\vec{\kappa}_1 = \vec{z} + \vec{\lambda}/2$. The functions y are the same as in (2.12) of [1] and the polynomial parts of the Fourier transforms in the second term of the integrand are given by eq. (2.9) of the same paper.

The Galilei-invariant versions of these matrix elements can be easily calculated, too. Instead of (2.12) we obtain with the projection operator \hat{C}_A out of eq. (1.7) of ref. [1]

$$\begin{aligned} \frac{\langle |\hat{O}_A^{\text{inv}} \hat{C}_A(0)| \rangle}{\langle |\hat{C}_A(0)| \rangle} &= \left(\frac{A}{4}\right)^{3/2} \sum_{12} \int d^3 \vec{k}_1 o_{12}(\vec{\kappa}_1, \vec{\lambda}) \frac{1}{\pi \sqrt{\pi}} \\ &\cdot \int d^3 \vec{\alpha} \left\langle |c_{\vec{k}_1 1}^\dagger c_{\vec{k}_1 - \vec{q} 2} \exp\{-i\vec{q} \cdot \vec{R}_A\} \exp\{i\vec{\alpha} \cdot b\hat{P}_A\}| \right\rangle = \\ &\left(\frac{A}{4}\right)^{3/2} \sum_{12} \int d^3 \vec{k}_1 o_{12}(\vec{\kappa}_1, \vec{\lambda}) \frac{1}{\pi \sqrt{\pi}} \\ &\cdot \int d^3 \vec{\alpha} \exp\left\{i \left[\vec{\kappa}_1 - \frac{A-1}{A} \vec{\lambda} \right] \cdot \vec{\alpha}\right\} \\ &\cdot \left\langle |c_{\vec{k}_1 1}^\dagger \exp\left\{-i \frac{A-1}{A} \vec{q} \cdot \vec{R}_{A-1}\right\} \right. \\ &\left. \cdot \exp\{i\vec{\alpha} \cdot b\hat{P}_{A-1}\} c_{\vec{k}_1 - \frac{A-1}{A} \vec{q} 2}| \right\rangle = \\ &\exp\left\{-\frac{1}{4} \frac{A-1}{A} \lambda^2\right\} \frac{1}{\pi \sqrt{\pi}} \\ &\cdot \int d^3 \vec{u} \exp\{-u^2\} \frac{1}{\pi \sqrt{\pi}} \int d^3 \vec{v} \exp\{-v^2\} \\ &\cdot \sum_1 o_{11} \left(\frac{i}{\sqrt{A}} \vec{u} - \vec{v} + \frac{A-1}{2A} \vec{\lambda}, \vec{\lambda} \right) x(\vec{\beta}_2', \vec{\beta}_1) = \\ &\exp\left\{-\frac{1}{4} \frac{A-1}{A} \lambda^2\right\} \frac{1}{\pi \sqrt{\pi}} \int d^3 \vec{u} \exp\{-u^2\} \frac{1}{\pi \sqrt{\pi}} \\ &\cdot \int d^3 \vec{v} \exp\{-v^2\} \sum_1 o_{11} \left(\frac{i}{\sqrt{A}} \vec{u} - \vec{v} + \frac{A-1}{2A} \vec{\lambda}, \vec{\lambda} \right) \\ &\cdot \begin{cases} 1 & \text{for } ^4\text{He} \\ 1 + 2v^2 - \lambda^2/2 & \text{for } ^{16}\text{O} \\ 5/2 + 2v^4 - \lambda^2 v^2 - \lambda^2 + \lambda^4/8 & \text{for } ^{40}\text{Ca} \end{cases}, \quad (2.14) \end{aligned}$$

where use has been made of the operator (2.27) from ref. [1] with $\vec{q}_1 = -\vec{\lambda}/A$ and $\vec{q}_2 = 0$ and of eq. (2.38) of ref. [1]. Furthermore,

$$\vec{\beta}_1 = -i\sqrt{2}\vec{v} + \frac{i}{\sqrt{2}}\vec{\lambda} \quad (2.15)$$

and

$$\vec{\beta}_2' = -i\sqrt{2}\vec{v} - \frac{i}{\sqrt{2}}\vec{\lambda}$$

have been used to evaluate the functions x out of eqs. (2.47), (2.50) and (2.53) out of ref. [1] for the three considered nuclei, respectively.

Note, that the functions x have here the same dependence on \vec{v} as the functions y in eq. (2.12) on \vec{z} . Thus, if the matrix elements $o_{12}(\vec{\kappa}_1, \vec{\lambda})$ do not depend on $\vec{\kappa}_1$ like it is the case for the charge density (2.3) (spin and convection currents do not contribute here because of the vanishing total angular momentum), the integral $(\pi\sqrt{\pi})^{-1} \int d^3\vec{u} \exp\{-u^2\}$ gives unity and we are left with

$$\frac{\langle |\hat{O}_A^{\text{inv}} \hat{C}_A(0)| \rangle}{\langle |\hat{C}_A(0)| \rangle} = \langle |\hat{O}| \rangle \exp\left\{ \frac{1}{4A} \lambda^2 \right\}. \quad (2.16)$$

This is due to the fact that $|\rangle = |\text{int}\rangle |(0s)_{\text{com}}\rangle$ is a “non-spurious” oscillator configuration which splits into an internal and a COM part with the COM in its oscillator ground state. Consequently,

$$\begin{aligned} \langle |\hat{O}| \rangle &= \langle \text{int} | \hat{O} \exp\{-i\vec{q} \cdot \vec{R}_A\} | \text{int} \rangle \\ &\cdot \langle (0s)_{\text{com}} | \exp\{+i\vec{q} \cdot \vec{R}_A\} | (0s)_{\text{com}} \rangle. \end{aligned} \quad (2.17)$$

From this (2.16) can be easily obtained. The exponential factor occurring in (2.16) is called the “Tassie-Barker factor” [3] and is widely used in the analysis of electron scattering. As has been shown by Schmid and Reinhard [5] it can also be derived from the Galilei-invariant result for general (non-oscillator) wave functions by applying subsequently a kind of “Gaussian overlap approximation” to the matrix elements of the shift and the Gartenhaus-Schwartz operator.

For the projected (but not yet normalized) version of the hole-hole matrix element (2.13) one obtains

$$\begin{aligned} \langle |b_{Hh}^\dagger \hat{O}_{A-1}^{\text{inv}} \hat{C}_{A-1}(0) b_{H'h'}| \rangle &= \\ b^3 \pi \sqrt{\pi} \sum_{12} \int d^3 \vec{k}_1 o_{12}(\vec{\kappa}_1, \vec{\lambda}) \frac{1}{\pi \sqrt{\pi}} & \\ \cdot \int d^3 \vec{\alpha} \left\langle |b_{Hh}^\dagger c_{\vec{k}_1}^\dagger c_{\vec{k}_1 - \vec{q}_2} \exp\{-i\vec{q} \cdot \vec{R}_{A-1}\} \right. & \\ \cdot \exp\{i\vec{\alpha} \cdot b \hat{P}_{A-1}\} b_{H'h'} | \rangle & \end{aligned}$$

$$\begin{aligned} b^3 \pi \sqrt{\pi} \sum_{12} \int d^3 \vec{k}_1 o_{12}(\vec{\kappa}_1, \vec{\lambda}) \frac{1}{\pi \sqrt{\pi}} \int d^3 \vec{\alpha} & \\ \cdot \exp\left\{ i \left[\vec{\kappa}_1 - \frac{A-2}{A-1} \vec{\lambda} \right] \cdot \vec{\alpha} \right\} & \\ \cdot \left\langle |b_{Hh}^\dagger c_{\vec{k}_1}^\dagger \exp\left\{ -i \frac{A-2}{A-1} \vec{q} \cdot \vec{R}_{A-2} \right\} \right. & \\ \cdot \exp\{i\vec{\alpha} \cdot b \hat{P}_{A-2}\} c_{\vec{k}_1 - \frac{A-2}{A-1} \vec{q}_2} b_{H'h'} | \rangle & = \\ \exp\left\{ -\frac{1}{4} \frac{A-2}{A-1} \lambda^2 \right\} \left(\frac{4}{A-1} \right)^{3/2} & \\ \cdot b^3 \pi \sqrt{\pi} \frac{1}{\pi \sqrt{\pi}} \int d^3 \vec{u} \exp\{-u^2\} & \\ \cdot \frac{1}{\pi \sqrt{\pi}} \int d^3 \vec{v} \exp\{-v^2\} & \\ \cdot \sum_{12} o_{12} \left(\frac{i}{\sqrt{A-1}} \vec{u} - \vec{v} + \frac{1}{2} \frac{A-2}{A-1} \vec{\lambda}, \vec{\lambda} \right) & \\ \cdot \left[\Delta_{21} \Delta_{h'h} z_{H'H}^{-1}(\vec{\beta}, \vec{\beta}') x(\vec{\beta}_2', \vec{\beta}_1) \right. & \\ \left. - \Delta_{1h'} \Delta_{2h} \tilde{r}_{H'}(\vec{\beta}_1, \vec{\beta}') r_H(\vec{\beta}_2', \vec{\beta}) \right], & \quad (2.18) \end{aligned}$$

where we have used again the operator (2.27) from ref. [1] with $\vec{q}_1 = -\vec{q}/A$ and $\vec{q}_2 = 0$ as well as eqs. (2.34) and (2.36) to (2.38) out of ref. [1]. Furthermore,

$$\begin{aligned} \vec{\beta} &\equiv \sqrt{\frac{2}{A-1}} \vec{u} + \frac{i}{\sqrt{2}} \frac{1}{A-1} \vec{\lambda}, \\ \vec{\beta}' &\equiv \sqrt{\frac{2}{A-1}} \vec{u} - \frac{i}{\sqrt{2}} \frac{1}{A-1} \vec{\lambda}, \\ \vec{\beta}_1 &\equiv -i\sqrt{2}\vec{v} + \frac{i}{\sqrt{2}} \vec{\lambda}, \\ \vec{\beta}_2' &\equiv -i\sqrt{2}\vec{v} - \frac{i}{\sqrt{2}} \vec{\lambda}, \end{aligned} \quad (2.19)$$

while \mathbf{z}^{-1} , $\tilde{\mathbf{r}}$, \mathbf{r} and x are given by eqs. (2.43) to (2.45) and (2.47) to (2.53) from ref. [1].

For H and H' both out of the last major shell occupied in $|\rangle$, we have $z_{H'H}^{-1} = \delta_{H'H}$ and $\tilde{r}_{H'}(\vec{\beta}_1, \vec{\beta}') = \tilde{r}_{H'}(\vec{\beta}_1)$ while $r_H(\vec{\beta}_2', \vec{\beta}) = r_H(\vec{\beta}_2')$. The only dependence on \vec{u} is then in the matrix elements o_{12} . Consequently, for o_{12} not depending on $\vec{\kappa}_1$ like it is the case for the charge density (2.3) and the spin current (2.9) or only linearly depending on this quantity like for the convection current (2.7) $(\pi\sqrt{\pi})^{-1} \int d^3\vec{u} \exp\{-u^2\}$ gives unity again. Using the normalisations out of subsect. 2.4 of ref. [1] for holes in the last occupied shell, we obtain immediately

$$\begin{aligned} \frac{\langle |b_{Hh}^\dagger \hat{O}_{A-1}^{\text{inv}} \hat{C}_{A-1}(0) b_{H'h'}| \rangle}{\sqrt{\langle |b_{Hh}^\dagger \hat{C}_{A-1}(0) b_{Hh}| \rangle \langle |b_{H'h'}^\dagger \hat{C}_{A-1}(0) b_{H'h'}| \rangle}} &= \\ \langle |b_{Hh}^\dagger \hat{O} b_{H'h'}| \rangle \exp\left\{ \frac{1}{4(A-1)} \lambda^2 \right\}. & \quad (2.20) \end{aligned}$$

As can be seen easily (2.20) holds only for both holes being “non-spurious” but not if at least one hole has an excitation energy $\geq 1\hbar\omega$.

Obviously for a fair comparison, the Tassie-Barker factor should be included in the “normal” results for all the form factors. This will be done throughout the following section.

2.2 Form factors

For the elastic electron scattering from the oscillator ground-state configurations for ${}^4\text{He}$, ${}^{16}\text{O}$ and ${}^{40}\text{Ca}$ obviously only the charge density operator does contribute. Furthermore, the energy transfer is here given by the recoil energy $(\hbar c\vec{q})^2/(2AMc^2)$ so that here

$$Q^2 = (\hbar c\vec{q})^2 \left\{ 1 - \frac{(\hbar c\vec{q})^2}{4A^2M^2c^4} \right\}. \quad (2.21)$$

Making use of (2.3) and (2.16) we obtain, evaluating (2.12),

$$\begin{aligned} F_{\text{ch,A}}^{\text{nor}}(Q^2) &\equiv \langle |\hat{\rho}| \rangle \exp \left\{ \frac{\lambda^2}{4A} \right\} = \\ F_{\text{ch,A}}^{\text{pro}}(Q^2) &\equiv \frac{\langle |\hat{\rho} \exp\{-i\vec{q} \cdot \vec{R}_A\} \hat{C}_A(0)| \rangle}{\langle |\hat{C}_A(0)| \rangle} = \\ &\exp \left\{ -\frac{1}{4} \frac{A-1}{A} \lambda^2 \right\} Z [f_p(Q^2) + f_n(Q^2)] \\ &\cdot \left\{ \begin{array}{ll} 1 & \text{for } {}^4\text{He} \\ 1 - \frac{1}{8} \lambda^2 & \text{for } {}^{16}\text{O} \\ 1 - \frac{1}{4} \lambda^2 + \frac{1}{80} \lambda^4 & \text{for } {}^{40}\text{Ca} \end{array} \right\} \equiv \\ &\exp \left\{ -\frac{1}{4} \frac{A-1}{A} \lambda^2 \right\} Z \Phi_A(\lambda), \end{aligned} \quad (2.22)$$

since $N = Z$ in these nuclei. The shorthand notation $\Phi_A(\lambda)$ has been introduced here for later use. For the scattering from the one-hole state Hh to the one-hole state $H'h'$ we have, instead of (2.21),

$$Q^2 = (\hbar c\vec{q})^2 - \left(\frac{(\hbar c\vec{q})^2}{2(A-1)Mc^2} + |E_{Hh} - E_{H'h'}| \right)^2. \quad (2.23)$$

Since for all form factors discussed a $\delta_{\tau_h \tau_{h'}}$ is obtained we shall always assume that $\tau_h = \tau_{h'} = \tau$ in the following.

As already mentioned, holes out of the last occupied shell are non-spurious again. The corresponding form factors can thus be calculated in the usual way or copied from the literature (see, *e.g.*, [9]). However, for completeness we shall list these results in the appendix.

In the present context obviously the matrix elements between holes with spurious admixtures are more interesting. We shall start with the cases where both holes are out of the same major shell.

For the $0s$ holes in ${}^{16}\text{O}$ we obtain without projection

$$\begin{aligned} F_{\text{ch,nor}}^{0s_{1/2m}, 0s_{1/2m'}}(Q^2) &= \\ \exp \left\{ -\frac{7}{30} \lambda^2 \right\} \delta_{m'm} [8\Phi_{16}(\lambda) - f_\tau(Q^2)] \end{aligned} \quad (2.24)$$

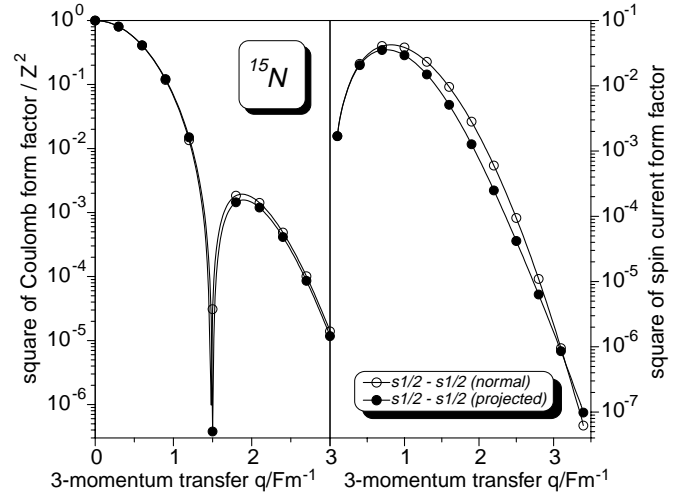


Fig. 1. The left side of the figure displays the square of the Coulomb form factor divided by Z^2 for the “elastic” electron scattering from the $0s$ proton hole in ${}^{16}\text{O}$ as a function of the 3-momentum transfer q . Compared are the normal approach (open circles) including the Tassie-Barker factor and the full Galilei-invariant result (full circles). On the right side the square of the spin current form factor for the scattering from the $0s$ proton hole in ${}^{16}\text{O}$ with spin-flip is presented.

and

$$\begin{aligned} F_{\text{sc}, \pm 1, \text{nor}}^{0s_{1/2m}, 0s_{1/2m'}}(Q^2) &= \\ \delta_{m' \pm 1/2} \delta_{m \mp 1/2} \exp \left\{ -\frac{7}{30} \lambda^2 \right\} \frac{\lambda}{\sqrt{2}} \frac{G_M^\tau(Q^2) \hbar c}{Mc^2 b}, \end{aligned} \quad (2.25)$$

while the Galilei-invariant results are here

$$\begin{aligned} F_{\text{ch,pro}}^{0s_{1/2m}, 0s_{1/2m'}}(Q^2) &= \delta_{m'm} \exp \left\{ -\frac{7}{30} \lambda^2 \right\} \\ &\cdot \left[8\Phi_{16}(\lambda) \left\{ 1 - \frac{1}{360} \lambda^2 \right\} - f_\tau(Q^2) \left\{ 1 - \frac{2}{45} \lambda^2 + \frac{1}{720} \lambda^4 \right\} \right] \end{aligned} \quad (2.26)$$

and

$$\begin{aligned} F_{\text{sc}, \pm 1, \text{pro}}^{0s_{1/2m}, 0s_{1/2m'}}(Q^2) &= \\ \delta_{m' \pm 1/2} \delta_{m \mp 1/2} \exp \left\{ -\frac{7}{30} \lambda^2 \right\} \frac{G_M^\tau(Q^2) \hbar c}{Mc^2 b} \frac{\lambda}{\sqrt{2}} \\ \cdot \left\{ 1 - \frac{2}{45} \lambda^2 + \frac{1}{720} \lambda^4 \right\}, \end{aligned} \quad (2.27)$$

respectively.

Figure 1 shows on the left side the squares of the charge form factors (2.24) and (2.26) for the nucleus ${}^{15}\text{N}$ (both divided by $Z^2 = 49$) and on the right the squares of the corresponding spin current form factors (2.25) and (2.27). Since it is not the aim of the present paper to compare with experimental data but rather to investigate the effects of the restoration of Galilei invariance, the nucleon form factors have been taken in the $q \rightarrow 0$ limit (*i.e.*, one for the proton and zero for the neutron version of (2.4) and

+2.793 for the proton and -1.913 for the neutron magnetic Sachs form factor out of (2.5) entering the expressions for the spin current). As can be seen, the COM projected charge form factor is almost identical to the Tassie-Barker corrected normal one up to about 1.5 inverse Fm, while at higher momentum transfers the normal description yields a slight overestimation of the strength. In the spin current form factor the effects are larger. The reason for this is that the charge form factor is dominated by the first term in (2.24) corresponding to the elastic scattering from the parent nucleus ^{16}O which gets only a small correction in (2.26). For the spin current this term is absent. Here we see only the ‘‘hole term’’ which gets a larger correction due to the restoration of Galilei invariance.

Rather similar effects can be seen for the same transition in ^{40}Ca . Here the normal results are

$$F_{\text{ch, nor}}^{0s_{1/2m}, 0s_{1/2m'}}(Q^2) = \exp\left\{-\frac{19}{78}\lambda^2\right\} \delta_{m'm} [20\Phi_{40}(\lambda) - f_\tau(Q^2)] \quad (2.28)$$

and

$$F_{\text{sc}, \pm 1, \text{nor}}^{0s_{1/2m}, 0s_{1/2m'}}(Q^2) = \delta_{m' \pm 1/2} \delta_{m \mp 1/2} \cdot \exp\left\{-\frac{19}{78}\lambda^2\right\} \frac{\lambda}{\sqrt{2}} \frac{G_M^\tau(Q^2)\hbar c}{Mc^2b}, \quad (2.29)$$

while with projection into the COM rest frame one obtains

$$F_{\text{ch, pro}}^{0\bar{s}_{1/2m}, 0\bar{s}_{1/2m'}}(Q^2) = \delta_{m'm} \exp\left\{-\frac{19}{78}\lambda^2\right\} \cdot \left[20\Phi_{40}(\lambda) \left\{1 - \frac{7}{21996}\lambda^2 + \frac{1}{17156880}\lambda^4\right\} - f_\tau(Q^2) \left\{1 - \frac{70}{5499}\lambda^2 + \frac{121}{1715688}\lambda^4 - \frac{1}{17156880}\lambda^6 + \frac{1}{137255040}\lambda^8\right\}\right] \quad (2.30)$$

and

$$F_{\text{sc}, \pm 1, \text{pro}}^{0\bar{s}_{1/2m}, 0\bar{s}_{1/2m'}}(Q^2) = \delta_{m' \pm 1/2} \delta_{m \mp 1/2} \cdot \exp\left\{-\frac{19}{78}\lambda^2\right\} \frac{G_M^\tau(Q^2)\hbar c}{Mc^2b} \frac{\lambda}{\sqrt{2}} \cdot \left\{1 - \frac{70}{5499}\lambda^2 + \frac{121}{1715688}\lambda^4 - \frac{1}{17156880}\lambda^6 + \frac{1}{137255040}\lambda^8\right\}. \quad (2.31)$$

The squares of the form factors (2.28) to (2.31) (again for a proton hole and with the nucleon form factors in the $q \rightarrow 0$ limit) are presented in fig. 2. Here the Tassie-Barker corrected normal and the projected charge form factor are almost identical. In the spin current results comparable differences are seen as in case of ^{15}N .

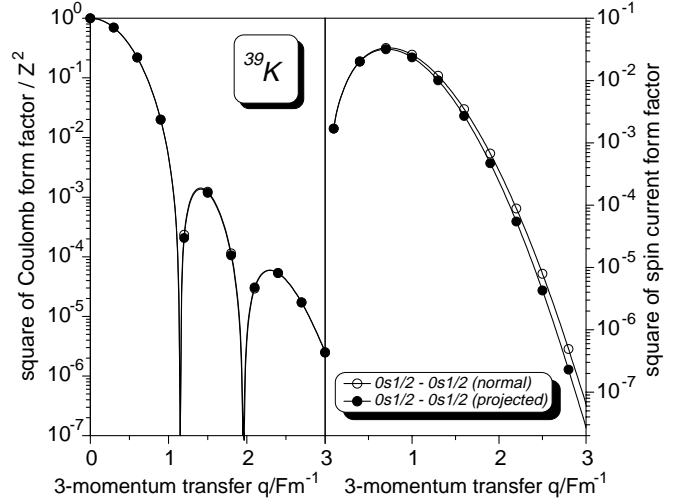


Fig. 2. Same as in fig. 1, but for the scattering from the $0s$ proton hole in ^{40}Ca .

In ^{40}Ca we can furthermore consider the scattering between the $0p$ holes. Here we obtain in the normal case

$$F_{\text{ch, nor}}^{0p_{jm}, 0p_{j'm'}}(Q^2) = \delta_{m'm} \exp\left\{-\frac{19}{78}\lambda^2\right\} \cdot \left[\delta_{j'j} \left\{20\Phi_{40}(\lambda) - f_\tau(Q^2) \left[1 - \frac{1}{6}\lambda^2\right]\right\} + f_\tau(Q^2) \frac{1}{6}\lambda^2 (-)^{m-1/2} \sqrt{(2j+1)(2j'+1)} \cdot (jj'2|m-m0)(jj'2|1/2-1/20)\right], \quad (2.32)$$

while

$$F_{\text{sc}, \pm 1, \text{nor}}^{0p_{jm}, 0p_{j'm'}}(Q^2) = \frac{G_M^\tau(Q^2)\hbar c}{Mc^2b} \exp\left\{-\frac{19}{78}\lambda^2\right\} \frac{\lambda}{\sqrt{2}} \cdot \left[\delta_{j'3/2} \delta_{j'3/2} \left\{[\delta_{m' \pm 3/2} \delta_{m \pm 1/2} + \delta_{m' \mp 1/2} \delta_{m \mp 3/2}] \cdot \frac{1}{\sqrt{3}} + \delta_{m' \pm 1/2} \delta_{m \mp 1/2} \frac{2}{3} \left[1 - \frac{1}{2}\lambda^2\right]\right\} - \delta_{j'1/2} \delta_{j'1/2} \left\{\delta_{m' \pm 1/2} \delta_{m \mp 1/2} \frac{1}{3} \left[1 - \frac{1}{2}\lambda^2\right]\right\} \mp \delta_{j'1/2} \delta_{j'3/2} \left\{\delta_{m' \pm 3/2} \delta_{m \pm 1/2} \sqrt{\frac{2}{3}} + \delta_{m' \pm 1/2} \delta_{m \mp 1/2} \frac{\sqrt{2}}{3} \left[1 - \frac{1}{2}\lambda^2\right]\right\} \pm \delta_{j'3/2} \delta_{j'1/2} \left\{\delta_{m' \mp 1/2} \delta_{m \mp 3/2} \sqrt{\frac{2}{3}} + \delta_{m' \pm 1/2} \delta_{m \mp 1/2} \frac{\sqrt{2}}{3} \left[1 - \frac{1}{2}\lambda^2\right]\right\}\right] \quad (2.33)$$

and the convection current yields

$$\begin{aligned}
F_{\text{cc}, \pm 1, \text{nor}}^{0p_{jm}, 0p_{j'm'}}(Q^2) &= \frac{f_{\tau}^{\text{cc}}(Q^2)\hbar c}{Mc^2b} \exp\left\{-\frac{19}{78}\lambda^2\right\} \frac{\lambda}{2} \\
&\cdot \left[\delta_{j\ 3/2}\delta_{j'\ 3/2} \left\{ [\delta_{m'\pm 3/2}\delta_{m\pm 1/2} + \delta_{m'\mp 1/2}\delta_{m\mp 3/2}] \right. \right. \\
&\cdot \left. \left. \sqrt{\frac{2}{3}} + \delta_{m'\pm 1/2}\delta_{m\mp 1/2} \frac{2\sqrt{2}}{3} \right\} \right. \\
&+ \delta_{j\ 1/2}\delta_{j'\ 1/2} \left\{ \delta_{m'\pm 1/2}\delta_{m\mp 1/2} \frac{2\sqrt{2}}{3} \right\} \pm \delta_{j\ 1/2}\delta_{j'\ 3/2} \\
&\cdot \left\{ \delta_{m'\pm 3/2}\delta_{m\pm 1/2} \frac{1}{\sqrt{3}} + \delta_{m'\pm 1/2}\delta_{m\mp 1/2} \frac{1}{3} \right\} \mp \delta_{j\ 3/2}\delta_{j'\ 1/2} \\
&\cdot \left. \left\{ \delta_{m'\mp 1/2}\delta_{m\mp 3/2} \frac{1}{\sqrt{3}} + \delta_{m'\pm 1/2}\delta_{m\mp 1/2} \frac{1}{3} \right\} \right], \quad (2.34)
\end{aligned}$$

which are, except for the different exponential and the different “elastic” term $\Phi_{40}(\lambda)$ in the charge form factor identical to the results (A.3) to (A.5) for the “non-spurious” $0p$ - $0p$ transition in the $A = 15$ system given in the appendix. With projection into the COM rest frame one gets, on the other hand,

$$\begin{aligned}
F_{\text{ch}, \text{pro}}^{0p_{jm}, 0p_{j'm'}}(Q^2) &= \delta_{m'm} \exp\left\{-\frac{19}{78}\lambda^2\right\} \\
&\cdot \left[\delta_{j'j} \left\{ 20\Phi_{40}(\lambda) \left[1 - \frac{2}{4095}\lambda^2 \right] - f_{\tau}(Q^2) \right. \right. \\
&\cdot \left. \left. \left[1 - \frac{305}{1638}\lambda^2 + \frac{1}{364}\lambda^4 - \frac{1}{32760}\lambda^6 \right] \right\} - \frac{281}{1638}\lambda^2 \right. \\
&\cdot \left. \left[\frac{16}{281}\Phi_{40}(\lambda) - f_{\tau}(Q^2) \left[1 - \frac{21}{1405}\lambda^2 + \frac{1}{5620}\lambda^4 \right] \right] \right. \\
&\cdot (-)^{m-1/2} \sqrt{(2j+1)(2j'+1)} \\
&\cdot \left. \left. (jj'2|m-m0)(jj'2|1/2-1/20) \right] \right], \quad (2.35)
\end{aligned}$$

while

$$\begin{aligned}
F_{\text{sc}, \pm 1, \text{pro}}^{0p_{jm}, 0p_{j'm'}}(Q^2) &= \exp\left\{-\frac{19}{78}\lambda^2\right\} \frac{G_M^{\tau}(Q^2)\hbar c}{Mc^2b} \frac{\lambda}{\sqrt{2}} \\
&\cdot \left[\delta_{j\ 3/2}\delta_{j'\ 3/2} \left\{ [\delta_{m'\pm 3/2}\delta_{m\pm 1/2} + \delta_{m'\mp 1/2}\delta_{m\mp 3/2}] \right. \right. \\
&\cdot \left. \left. \frac{1}{\sqrt{3}} \left[1 - \frac{4}{273}\lambda^2 + \frac{1}{5460}\lambda^4 \right] + \delta_{m'\pm 1/2}\delta_{m\mp 1/2} \right. \right. \\
&\cdot \left. \left. \frac{2}{3} \left[1 - \frac{289}{546}\lambda^2 + \frac{43}{5460}\lambda^4 - \frac{281}{2981160}\lambda^6 \right] \right\} \right. \\
&- \delta_{j\ 1/2}\delta_{j'\ 1/2} \left\{ \delta_{m'\pm 1/2}\delta_{m\mp 1/2} \frac{1}{3} \left[1 - \frac{289}{546}\lambda^2 \right. \right.
\end{aligned}$$

$$\begin{aligned}
&\left. \left. + \frac{43}{5460}\lambda^4 - \frac{281}{2981160}\lambda^6 \right] \right\} \mp \delta_{j\ 1/2}\delta_{j'\ 3/2} \\
&\cdot \left\{ \delta_{m'\pm 3/2}\delta_{m\pm 1/2} \sqrt{\frac{2}{3}} \left[1 - \frac{4}{273}\lambda^2 + \frac{1}{5460}\lambda^4 \right] \right. \\
&+ \delta_{m'\pm 1/2}\delta_{m\mp 1/2} \frac{\sqrt{2}}{3} \left[1 - \frac{289}{546}\lambda^2 + \frac{43}{5460}\lambda^4 \right. \\
&\left. \left. - \frac{281}{2981160}\lambda^6 \right] \right\} \pm \delta_{j\ 3/2}\delta_{j'\ 1/2} \left\{ \delta_{m'\mp 1/2}\delta_{m\mp 3/2} \right. \\
&\cdot \left. \sqrt{\frac{2}{3}} \left[1 - \frac{4}{273}\lambda^2 + \frac{1}{5460}\lambda^4 \right] + \delta_{m'\pm 1/2}\delta_{m\mp 1/2} \right. \\
&\cdot \left. \left. \frac{\sqrt{2}}{3} \left[1 - \frac{289}{546}\lambda^2 + \frac{43}{5460}\lambda^4 - \frac{281}{2981160}\lambda^6 \right] \right\} \right], \quad (2.36)
\end{aligned}$$

and

$$\begin{aligned}
F_{\text{cc}, \pm 1, \text{pro}}^{0p_{jm}, 0p_{j'm'}}(Q^2) &= \frac{\hbar c}{Mc^2b} \exp\left\{\frac{19}{78}\lambda^2\right\} \frac{281}{546}\lambda \\
&\cdot \left[\frac{4}{281}\Phi_{40}^{\text{cc}}(\lambda) - f_{\tau}^{\text{cc}}(Q^2) \left\{ 1 - \frac{21}{1405}\lambda^2 + \frac{1}{5620}\lambda^4 \right\} \right. \\
&\cdot \left[\delta_{j\ 3/2}\delta_{j'\ 3/2} \left\{ [\delta_{m'\pm 3/2}\delta_{m\pm 1/2} + \delta_{m'\mp 1/2}\delta_{m\mp 3/2}] \right. \right. \\
&\cdot \left. \left. \sqrt{\frac{2}{3}} + \delta_{m'\pm 1/2}\delta_{m\mp 1/2} \frac{2\sqrt{2}}{3} \right\} + \delta_{j\ 1/2}\delta_{j'\ 1/2} \right. \\
&\cdot \left\{ \delta_{m'\pm 1/2}\delta_{m\mp 1/2} \frac{2\sqrt{2}}{3} \right\} \pm \delta_{j\ 1/2}\delta_{j'\ 3/2} \\
&\cdot \left\{ \delta_{m'\pm 3/2}\delta_{m\pm 1/2} \frac{1}{\sqrt{3}} + \delta_{m'\pm 1/2}\delta_{m\mp 1/2} \frac{1}{3} \right\} \\
&\mp \delta_{j\ 3/2}\delta_{j'\ 1/2} \left\{ \delta_{m'\mp 1/2}\delta_{m\mp 3/2} \frac{1}{\sqrt{3}} + \delta_{m'\pm 1/2}\delta_{m\mp 1/2} \frac{1}{3} \right\} \right], \quad (2.37)
\end{aligned}$$

where we have introduced

$$\begin{aligned}
\Phi_A^{\text{cc}}(\lambda) &= [f_p^{\text{cc}}(Q^2) + f_n^{\text{cc}}(Q^2)] \\
&\cdot \left\{ \begin{array}{ll} 1 - \frac{1}{8}\lambda^2 & \text{for } A = 16 \\ 1 - \frac{1}{4}\lambda^2 + \frac{1}{80}\lambda^4 & \text{for } A = 40 \end{array} \right\} \quad (2.38)
\end{aligned}$$

in analogy to the definition (2.22).

Again the charge form factor is dominated by the term corresponding to the elastic scattering from ^{40}Ca which gets only a small correction in the COM projection. The charge form factors (2.33) and (2.35) are therefore again almost identical and not shown in the present paper. Figure 3 presents the squares of the convection and spin current form factors (naturally summed over the final states and averaged over the initial states) for a proton $0p_{3/2}$ hole as initial and final state again in the limit $q \rightarrow 0$. In both cases only small corrections are introduced by the projection.

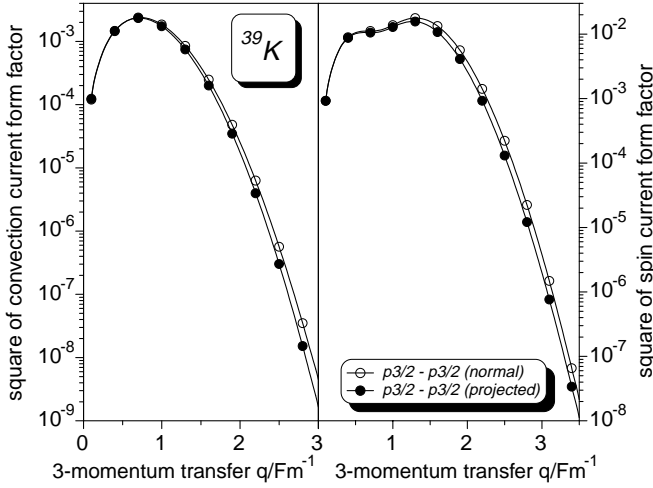


Fig. 3. The squares of the convection current (left side) and the spin current (right side) form factors are presented as functions of the 3-momentum transfer q for the electron scattering from the $0p_{3/2}$ proton hole state in ^{40}Ca to the same final state. Since the convection current changes the orbital angular momentum, the spin current the spin projection both are “inelastic” processes. Compared are the “normal” and the “projected” results.

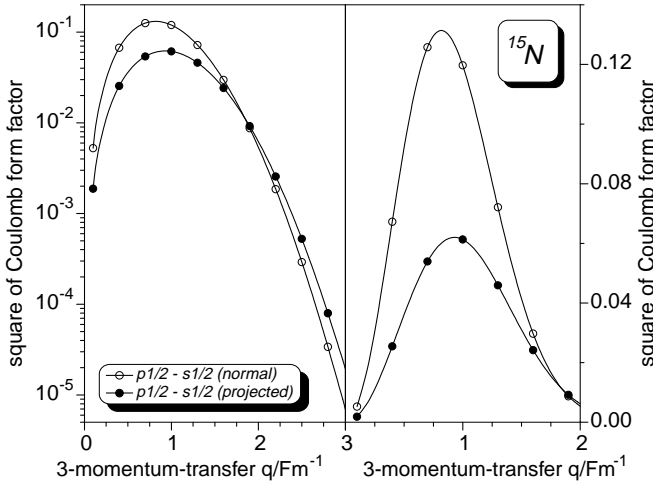


Fig. 4. The square of the Coulomb form factor in logarithmic (left side) and linear scale (right side) for the inelastic electron scattering from the $0p_{1/2}$ proton hole state in ^{16}O (i.e. the ground state of ^{15}N) to the $0s_{1/2}$ proton hole in the same nucleus (i.e. an $1\hbar\omega$ excited state of ^{15}N) are plotted versus the 3-momentum transfer. Again the results obtained with the normal approach are compared to those of the full Galilei-invariant description.

Next, we study holes which are separated by $1\hbar\omega$. For the scattering from the $0p$ to the $0s$ holes in ^{16}O we obtain in the normal case

$$F_{\text{ch, nor}}^{0s_{1/2m}, 0p_{j'm'}}(Q^2) = \delta_{m'm} f_{\tau}(Q^2) \exp\left\{-\frac{7}{30}\lambda^2\right\} \cdot \frac{i\lambda}{2} \sqrt{\frac{2j'+1}{3}} \left[\delta_{j'3/2} + (-)^{1/2-m} \delta_{j'1/2}\right], \quad (2.39)$$

while

$$F_{\text{sc, } \pm 1, \text{ nor}}^{0s_{1/2m}, 0p_{j'm'}}(Q^2) = -\delta_{m' \pm 1/2} \delta_{m \mp 1/2} \cdot \frac{G_M^{\tau}(Q^2) \hbar c}{Mc^2 b} \exp\left\{-\frac{7}{30}\lambda^2\right\} \cdot \frac{i\lambda^2}{2\sqrt{2}} \sqrt{\frac{2j'+1}{3}} \left[\delta_{j'3/2} \pm \delta_{j'1/2}\right] \quad (2.40)$$

and

$$F_{\text{cc, } \pm 1, \text{ nor}}^{0s_{1/2m}, 0p_{j'm'}}(Q^2) = -\frac{f_{\tau}^{\text{cc}}(Q^2) \hbar c}{Mc^2 b} \exp\left\{-\frac{7}{30}\lambda^2\right\} \cdot \frac{i}{\sqrt{2}} \left[\delta_{j'3/2} \left\{ \delta_{m' \pm 3/2} \delta_{m \pm 1/2} + \delta_{m' \pm 1/2} \delta_{m \mp 1/2} \frac{1}{\sqrt{3}} \right\} \mp \delta_{j'1/2} \delta_{m' \pm 1/2} \delta_{m \mp 1/2} \sqrt{\frac{2}{3}} \right]. \quad (2.41)$$

The corresponding projected results are

$$F_{\text{ch, pro}}^{0s_{1/2m}, 0p_{j'm'}}(Q^2) = -\delta_{m'm} \exp\left\{-\frac{7}{30}\lambda^2\right\} \cdot i \frac{8}{15} \sqrt{\frac{5}{4}} \lambda \sqrt{\frac{2j'+1}{3}} \left[\delta_{j'3/2} + (-)^{1/2-m} \delta_{j'1/2}\right] \cdot \left[\frac{1}{2} \Phi_{16}(\lambda) - f_{\tau}(Q^2) \left\{1 - \frac{1}{32}\lambda^2\right\}\right], \quad (2.42)$$

while

$$F_{\text{sc, } \pm 1, \text{ pro}}^{0s_{1/2m}, 0p_{j'm'}}(Q^2) = -\delta_{m' \pm 1/2} \delta_{m \mp 1/2} \cdot \frac{G_M^{\tau}(Q^2) \hbar c}{Mc^2 b} \exp\left\{-\frac{7}{30}\lambda^2\right\} \cdot \frac{i\lambda^2}{\sqrt{2}} \frac{8}{15} \sqrt{\frac{5}{4}} \sqrt{\frac{2j'+1}{3}} \left[\delta_{j'3/2} \pm \delta_{j'1/2}\right] \left\{1 - \frac{1}{32}\lambda^2\right\} \quad (2.43)$$

and

$$F_{\text{cc, } \pm 1, \text{ pro}}^{0s_{1/2m}, 0p_{j'm'}}(Q^2) = \frac{\hbar c}{Mc^2 b} \exp\left\{-\frac{7}{30}\lambda^2\right\} \frac{i}{\sqrt{2}} \frac{16}{15} \sqrt{\frac{5}{4}} \cdot \left[\delta_{j'3/2} \left\{ \delta_{m' \pm 3/2} \delta_{m \pm 1/2} + \delta_{m' \pm 1/2} \delta_{m \mp 1/2} \frac{1}{\sqrt{3}} \right\} \mp \delta_{j'1/2} \delta_{m' \pm 1/2} \delta_{m \mp 1/2} \sqrt{\frac{2}{3}} \right] \cdot \left[\frac{1}{2} \Phi_{16}^{\text{cc}}(\lambda) - f_{\tau}^{\text{cc}}(Q^2) \left\{1 - \frac{1}{32}\lambda^2\right\}\right]. \quad (2.44)$$

The results (2.39) up to (2.44) are summarized for the scattering from the $0p_{1/2}$ ground state to the $0s_{1/2}$ excited state in ^{15}N in figs. 4 to 6. Figure 4 displays the square of the Coulomb form factors without (2.39) and with projection (2.42) into the COM rest frame plotted in

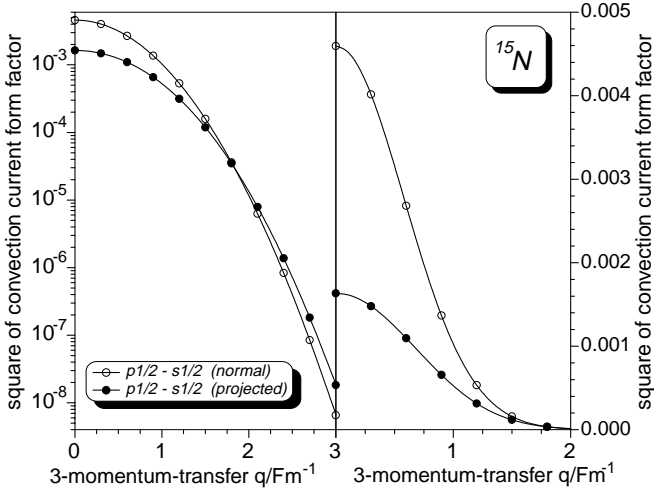


Fig. 5. Same as in fig. 4, but for the square of the convection current form factor.

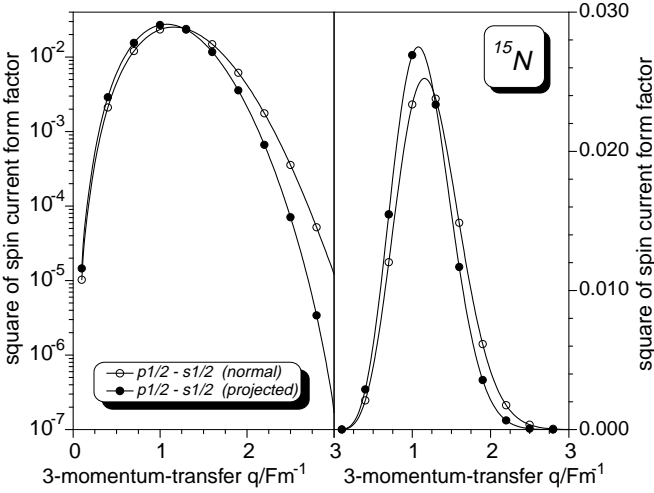


Fig. 6. Same as in fig. 4, but for the square of the spin current form factor.

a logarithmic (left side) and in a linear scale (right side). For this transition drastic differences are seen between the Tassie-Barker corrected normal and the full COM projected result. For low momentum transfer the normal description overestimates the correct Galilei-invariant strength by almost a factor of 2.5. At momentum transfers of more than two inverse Fm on the other hand the normal approach underestimates the strength considerably. The drastic effects at small momentum transfers are here due to the first term in (2.42) which corresponds to the elastic scattering from ^{16}O . This term, which removes the spurious admixtures, is absent in the normal description.

As can be seen from fig. 5, the drastic effects of the full restoration of Galilei invariance are seen for the square of the convection current form factor, too. Again the normal description (2.41) yields a dramatic overestimation of the projected strength (2.44) at low momentum transfer, while at momentum transfers above two inverse Fm an underestimation of the projected strength is obtained.

Again it is the “elastic term” in (2.44) which dominates these differences.

Finally, the squares of the spin current form factors (2.40) and (2.43) are presented in fig. 6. Here, as expected because of the absence of an “elastic term” in (2.43), the differences between the normal and the projected approach are rather small at low momentum transfers. At momentum transfers above two inverse Fm, however, the effects of the λ^2 term in (2.43) can clearly be seen. They lead to a considerable reduction of the normal strength. The absence of an “elastic term” (the occurrence of which caused the dramatic effects seen in the charge and convection current results) in the spin current form factor results from the fact that the spin current is always connected with a spin-flip. Such a spin-flip, however, cannot be induced by the COM motion which only causes “shifts” of the total wave function in ordinary space.

In ^{40}Ca we restrict ourselves in this section to the $0d-0p$ transitions. The form factors for the other $1\hbar\omega$ transitions are presented in the appendix.

Here we obtain in the normal approximation

$$\begin{aligned}
 F_{\text{ch, nor}}^{0p_{jm}, 0d_{j'm'}}(Q^2) &= \delta_{m'm} f_{\tau}(Q^2) \exp\left\{-\frac{19}{78}\lambda^2\right\} i\lambda \\
 &\cdot \left[\delta_{j\ 3/2} \delta_{j'\ 5/2} \left\{ \delta_{m\pm 3/2} \sqrt{\frac{2}{5}} + \delta_{m\pm 1/2} \sqrt{\frac{3}{5}} \left[1 - \frac{1}{6}\lambda^2\right] \right\} \right. \\
 &\pm \delta_{j\ 3/2} \delta_{j'\ 3/2} \left\{ \delta_{m\pm 3/2} \frac{1}{\sqrt{10}} + \delta_{m\pm 1/2} \frac{1}{3\sqrt{10}} [1 - \lambda^2] \right\} \\
 &\mp \delta_{j\ 1/2} \delta_{j'\ 5/2} \left\{ \delta_{m\pm 1/2} \frac{1}{2\sqrt{30}} \lambda^2 \right\} \\
 &\left. + \delta_{j\ 1/2} \delta_{j'\ 3/2} \left\{ \delta_{m\pm 1/2} \frac{\sqrt{5}}{3} \left[1 - \frac{1}{10}\lambda^2\right] \right\} \right], \quad (2.45)
 \end{aligned}$$

while

$$\begin{aligned}
 F_{\text{sc, } \pm 1, \text{ nor}}^{0p_{jm}, 0d_{j'm'}}(Q^2) &= -\frac{G_M^{\tau}(Q^2)\hbar c}{Mc^2b} \exp\left\{-\frac{19}{78}\lambda^2\right\} \frac{i\lambda^2}{\sqrt{2}} \\
 &\cdot \left[\delta_{j\ 3/2} \delta_{j'\ 5/2} \left\{ \delta_{m'\pm 3/2} \delta_{m\pm 1/2} \sqrt{\frac{2}{15}} + \delta_{m'\mp 3/2} \delta_{m\mp 1/2} \frac{1}{\sqrt{5}} \right. \right. \\
 &\left. \left. + \delta_{m'\pm 1/2} \delta_{m\mp 1/2} \frac{2}{\sqrt{15}} \left[1 - \frac{1}{4}\lambda^2\right] \right\} \pm \delta_{j\ 3/2} \delta_{j'\ 3/2} \right. \\
 &\cdot \left\{ \delta_{m'\pm 3/2} \delta_{m\pm 1/2} \frac{1}{\sqrt{30}} + \delta_{m'\mp 3/2} \delta_{m\mp 1/2} \sqrt{\frac{3}{10}} \right. \\
 &\left. \left. + \delta_{m'\pm 1/2} \delta_{m\mp 1/2} \frac{2}{3} \sqrt{\frac{2}{5}} \left[1 - \frac{1}{4}\lambda^2\right] \right\} \mp \delta_{j\ 1/2} \delta_{j'\ 5/2} \right. \\
 &\cdot \left\{ \delta_{m'\pm 3/2} \delta_{m\pm 1/2} \frac{2}{\sqrt{15}} + \delta_{m'\pm 1/2} \delta_{m\mp 1/2} \right. \\
 &\left. \cdot \sqrt{\frac{2}{15}} \left[1 - \frac{1}{4}\lambda^2\right] \right\} - \delta_{j\ 1/2} \delta_{j'\ 3/2} \left\{ \delta_{m'\pm 3/2} \delta_{m\pm 1/2} \frac{1}{\sqrt{15}} \right. \\
 &\left. \left. + \delta_{m'\pm 1/2} \delta_{m\mp 1/2} \frac{2}{3\sqrt{5}} \left[1 - \frac{1}{4}\lambda^2\right] \right\} \right] \quad (2.46)
 \end{aligned}$$

and

$$\begin{aligned}
F_{cc, \pm 1, \text{nor}}^{0p_{jm}, 0d_{j'm'}}(Q^2) = & -\frac{f_{\tau}^{cc}(Q^2)\hbar c}{Mc^2b} \exp\left\{-\frac{19}{78}\lambda^2\right\} i \\
& \cdot \left[\delta_{j\ 3/2}\delta_{j'\ 5/2} \left\{ \delta_{m'\pm 3/2}\delta_{m\pm 1/2} \sqrt{\frac{3}{5}} \left[1 - \frac{1}{3}\lambda^2\right] \right. \right. \\
& + \delta_{m'\mp 3/2}\delta_{m\mp 1/2} \frac{1}{\sqrt{10}} \left[1 - \frac{1}{2}\lambda^2\right] + \delta_{m'\pm 5/2}\delta_{m\pm 3/2} \\
& \left. \left. + \delta_{m'\pm 1/2}\delta_{m\mp 1/2} \sqrt{\frac{3}{10}} \left[1 - \frac{1}{2}\lambda^2\right] \right\} \right. \\
& \mp \delta_{j\ 3/2}\delta_{j'\ 3/2} \left\{ \delta_{m'\pm 3/2}\delta_{m\pm 1/2} \frac{1}{\sqrt{15}} \left[1 + \frac{1}{2}\lambda^2\right] \right. \\
& + \delta_{m'\mp 3/2}\delta_{m\mp 1/2} \frac{1}{\sqrt{15}} \left[1 - \frac{1}{2}\lambda^2\right] \\
& \left. \left. + \delta_{m'\pm 1/2}\delta_{m\mp 1/2} \frac{2}{3\sqrt{5}} \left[1 - \frac{1}{2}\lambda^2\right] \right\} \right. \\
& \mp \delta_{j\ 1/2}\delta_{j'\ 5/2} \left\{ \delta_{m'\pm 3/2}\delta_{m\pm 1/2} \frac{1}{\sqrt{30}} \lambda^2 \right\} \\
& + \delta_{j\ 1/2}\delta_{j'\ 3/2} \left\{ \delta_{m'\pm 3/2}\delta_{m\pm 1/2} \sqrt{\frac{5}{6}} \left[1 - \frac{1}{10}\lambda^2\right] \right. \\
& \left. \left. + \delta_{m'\pm 1/2}\delta_{m\mp 1/2} \frac{1}{3} \sqrt{\frac{5}{2}} \left[1 - \frac{1}{2}\lambda^2\right] \right\} \right]. \quad (2.47)
\end{aligned}$$

With projection into the COM rest frame we obtain, on the other hand,

$$\begin{aligned}
F_{\text{ch, pro}}^{0p_{jm}, 0d_{j'm'}}(Q^2) = & -\delta_{m'm} \exp\left\{-\frac{19}{78}\lambda^2\right\} i\lambda \frac{40}{\sqrt{1365}} \\
& \cdot \left[\delta_{j\ 3/2}\delta_{j'\ 5/2} \left\{ \delta_{m\pm 3/2} \sqrt{\frac{2}{5}} \left\{ \frac{1}{2} \Phi_{40}(\lambda) - f_{\tau} \left[1 - \frac{1}{80}\lambda^2\right] \right\} \right. \right. \\
& + \delta_{m\pm 1/2} \sqrt{\frac{3}{5}} \left\{ \frac{1}{2} \Phi_{40}(\lambda) - f_{\tau} \left[1 - \frac{11}{60}\lambda^2 + \frac{1}{480}\lambda^4\right] \right\} \left. \right\} \\
& \pm \delta_{j\ 3/2}\delta_{j'\ 3/2} \left\{ \delta_{m\pm 3/2} \frac{1}{\sqrt{10}} \left\{ \frac{1}{2} \Phi_{40}(\lambda) - f_{\tau} \left[1 - \frac{1}{80}\lambda^2\right] \right\} \right. \\
& + \delta_{m\pm 1/2} \frac{1}{3\sqrt{10}} \left\{ \frac{1}{2} \Phi_{40}(\lambda) - f_{\tau} \left[1 - \frac{83}{80}\lambda^2 + \frac{1}{80}\lambda^4\right] \right\} \left. \right\} \\
& \pm \delta_{j\ 1/2}\delta_{j'\ 5/2} \left\{ \delta_{m\pm 1/2} f_{\tau} \frac{41}{80\sqrt{30}} \lambda^2 \left[1 - \frac{1}{82}\lambda^2\right] \right\} \\
& + \delta_{j\ 1/2}\delta_{j'\ 3/2} \left\{ \delta_{m\pm 1/2} \frac{\sqrt{5}}{3} \right. \\
& \left. \left. \cdot \left\{ \frac{1}{2} \Phi_{40}(\lambda) - f_{\tau} \left[1 - \frac{23}{200}\lambda^2 + \frac{1}{800}\lambda^4\right] \right\} \right\} \right]. \quad (2.48)
\end{aligned}$$

Furthermore,

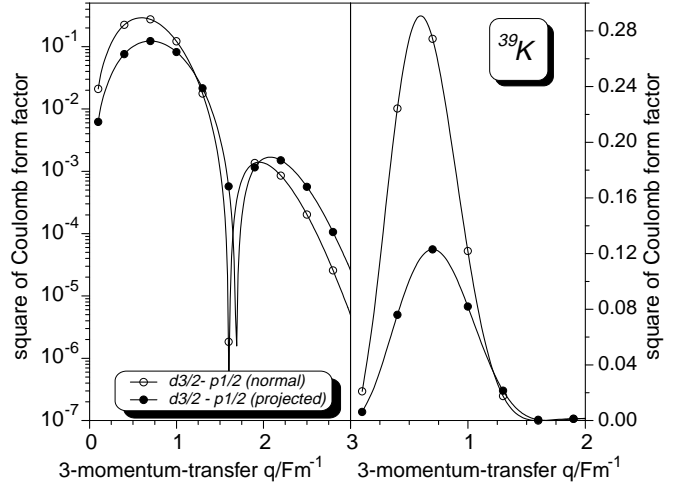


Fig. 7. The square of the Coulomb form factor in logarithmic (left side) and linear scale (right side) for the inelastic electron scattering from the $0d_{3/2}$ proton hole state in ^{40}O (*i.e.* the ground state of ^{39}K) to the $0p_{1/2}$ proton hole in the same nucleus (*i.e.* an $1\hbar\omega$ excited state of ^{39}K) are plotted *versus* the 3-momentum transfer. Again the results obtained with the normal approach are compared to those of the full Galilei-invariant description.

$$\begin{aligned}
F_{\text{sc, } \pm 1, \text{pro}}^{0p_{jm}, 0d_{j'm'}}(Q^2) = & -\frac{G_M^{\tau}(Q^2)\hbar c}{Mc^2b} \\
& \cdot \exp\left\{-\frac{19}{78}\lambda^2\right\} \frac{i\lambda^2}{\sqrt{2}} \frac{40}{\sqrt{1365}} \\
& \cdot \left[\delta_{j\ 3/2}\delta_{j'\ 5/2} \left\{ \delta_{m'\pm 3/2}\delta_{m\pm 1/2} \sqrt{\frac{2}{15}} \left[1 - \frac{\lambda^2}{80}\right] \right. \right. \\
& + \delta_{m'\mp 3/2}\delta_{m\mp 1/2} \frac{1}{\sqrt{5}} \left[1 - \frac{\lambda^2}{80}\right] \\
& \left. \left. + \delta_{m'\pm 1/2}\delta_{m\mp 1/2} \frac{2}{\sqrt{15}} \left[1 - \frac{43}{160}\lambda^2 + \frac{1}{320}\lambda^4\right] \right\} \right. \\
& \pm \delta_{j\ 3/2}\delta_{j'\ 3/2} \left\{ \delta_{m'\pm 3/2}\delta_{m\pm 1/2} \frac{1}{\sqrt{30}} \left[1 - \frac{\lambda^2}{80}\right] \right. \\
& + \delta_{m'\mp 3/2}\delta_{m\mp 1/2} \sqrt{\frac{3}{10}} \left[1 - \frac{\lambda^2}{80}\right] \\
& \left. \left. + \delta_{m'\pm 1/2}\delta_{m\mp 1/2} \frac{2}{3} \sqrt{\frac{2}{5}} \left[1 - \frac{43}{160}\lambda^2 + \frac{1}{320}\lambda^4\right] \right\} \right. \\
& \mp \delta_{j\ 1/2}\delta_{j'\ 5/2} \left\{ \delta_{m'\pm 3/2}\delta_{m\pm 1/2} \frac{2}{\sqrt{15}} \left[1 - \frac{\lambda^2}{80}\right] \right. \\
& + \delta_{m'\pm 1/2}\delta_{m\mp 1/2} \sqrt{\frac{2}{15}} \left[1 - \frac{43}{160}\lambda^2 + \frac{1}{320}\lambda^4\right] \left. \right\} \\
& - \delta_{j\ 1/2}\delta_{j'\ 3/2} \left\{ \delta_{m'\pm 3/2}\delta_{m\pm 1/2} \frac{1}{\sqrt{15}} \left[1 - \frac{\lambda^2}{80}\right] \right. \\
& \left. \left. + \delta_{m'\pm 1/2}\delta_{m\mp 1/2} \frac{2}{3\sqrt{5}} \left[1 - \frac{43}{160}\lambda^2 + \frac{1}{320}\lambda^4\right] \right\} \right]. \quad (2.49)
\end{aligned}$$

and

$$\begin{aligned}
F_{cc, \pm 1, \text{pro}}^{0p_{j m}, 0d_{j' m'}}(Q^2) &= \frac{\hbar c}{M c^2 b} \exp\left\{-\frac{19}{78}\lambda^2\right\} i \frac{40}{\sqrt{1365}} \\
&\cdot \left[\delta_{j \ 3/2} \delta_{j' \ 5/2} \left\{ \delta_{m' \pm 3/2} \delta_{m \pm 1/2} \sqrt{\frac{3}{5}} \right. \right. \\
&\cdot \left. \left. \left\{ \frac{1}{2} \Phi_{40}^{cc}(\lambda) - f_{\tau}^{cc} \left[1 - \frac{83}{240}\lambda^2 + \frac{\lambda^4}{240} \right] \right\} \right. \right. \\
&+ \delta_{m' \mp 3/2} \delta_{m \mp 1/2} \frac{1}{\sqrt{10}} \\
&\cdot \left. \left. \left\{ \frac{1}{2} \Phi_{40}^{cc}(\lambda) - f_{\tau}^{cc} \left[1 - \frac{43}{80}\lambda^2 + \frac{\lambda^4}{160} \right] \right\} \right. \right. \\
&+ \delta_{m' \pm 5/2} \delta_{m \pm 3/2} \left. \left. \left\{ \frac{1}{2} \Phi_{40}^{cc}(\lambda) - f_{\tau}^{cc} \left[1 - \frac{\lambda^2}{80} \right] \right\} \right. \right. \\
&+ \delta_{m' \pm 1/2} \delta_{m \mp 1/2} \sqrt{\frac{3}{10}} \\
&\cdot \left. \left. \left\{ \frac{1}{2} \Phi_{40}^{cc}(\lambda) - f_{\tau}^{cc} \left[1 - \frac{25}{48}\lambda^2 + \frac{\lambda^4}{160} \right] \right\} \right\} \right. \\
&\mp \delta_{j \ 3/2} \delta_{j' \ 3/2} \left. \left. \left\{ \delta_{m' \pm 3/2} \delta_{m \pm 1/2} \frac{1}{\sqrt{15}} \right. \right. \right. \\
&\cdot \left. \left. \left. \left\{ \frac{1}{2} \Phi_{40}^{cc}(\lambda) - f_{\tau}^{cc} \left[1 + \frac{39}{80}\lambda^2 - \frac{\lambda^4}{160} \right] \right\} \right. \right. \right. \\
&+ \delta_{m' \mp 3/2} \delta_{m \mp 1/2} \frac{1}{\sqrt{15}} \\
&\cdot \left. \left. \left. \left\{ \frac{1}{2} \Phi_{40}^{cc}(\lambda) - f_{\tau}^{cc} \left[1 - \frac{43}{80}\lambda^2 + \frac{\lambda^4}{160} \right] \right\} \right. \right. \right. \\
&+ \delta_{m' \pm 1/2} \delta_{m \mp 1/2} \frac{2}{3\sqrt{5}} \\
&\cdot \left. \left. \left. \left\{ \frac{1}{2} \Phi_{40}^{cc}(\lambda) - f_{\tau}^{cc} \left[1 - \frac{1}{2}\lambda^2 + \frac{\lambda^4}{160} \right] \right\} \right. \right. \right. \\
&\mp \delta_{j \ 1/2} \delta_{j' \ 5/2} \left. \left. \left\{ \delta_{m' \pm 3/2} \delta_{m \pm 1/2} \frac{1}{\sqrt{30}} \right. \right. \right. \\
&\cdot \left. \left. \left. \left\{ \frac{1}{2} \Phi_{40}^{cc}(\lambda) - f_{\tau}^{cc} \lambda^2 \left[1 - \frac{\lambda^2}{80} \right] \right\} - \delta_{m' \pm 1/2} \delta_{m \mp 1/2} \frac{\lambda^2}{40\sqrt{15}} \right\} \right. \right. \\
&+ \delta_{j \ 1/2} \delta_{j' \ 3/2} \left. \left. \left\{ \delta_{m' \pm 3/2} \delta_{m \pm 1/2} \sqrt{\frac{5}{6}} \right. \right. \right. \\
&\cdot \left. \left. \left. \left\{ \frac{1}{2} \Phi_{40}^{cc}(\lambda) - f_{\tau}^{cc} \left[1 - \frac{9}{80}\lambda^2 + \frac{\lambda^4}{800} \right] \right\} \right. \right. \right. \\
&+ \delta_{m' \pm 1/2} \delta_{m \mp 1/2} \frac{1}{3} \sqrt{\frac{5}{2}} \\
&\cdot \left. \left. \left. \left\{ \frac{1}{2} \Phi_{40}^{cc}(\lambda) - f_{\tau}^{cc} \left[1 - \frac{209}{400}\lambda^2 + \frac{\lambda^4}{160} \right] \right\} \right\} \right\} \right\}. \quad (2.50)
\end{aligned}$$

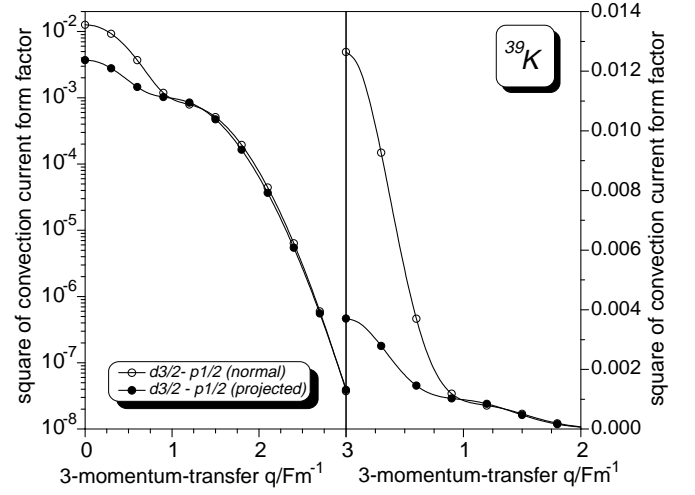


Fig. 8. Same as in fig. 7, but for the square of the convection current form factor.

The results (2.45) up to (2.50) are summarized for the scattering from the $0d_{3/2}$ ground state to the $0p_{1/2}$ excited state in ^{39}K in figs. 7 to 9. Figure 7 displays the square of the Coulomb form factors without (2.45) and with projection (2.48) into the COM rest frame plotted in a logarithmic (left side) and in a linear scale (right side). Again drastic differences are seen between the Tassie-Barker corrected normal and the full COM projected result. Comparison with fig. 4 clearly shows that these differences are of the same size as observed for the $1\hbar\omega$ transition in ^{15}N and thus are obviously not an $1/A$ effect. Again the normal description overestimates the correct Galilei-invariant strength at low momentum transfer by a factor of about 2.5, while at momentum transfers of more than about 1.2 inverse Fm the situation is reversed.

As already observed for ^{15}N , the drastic effects of the full restoration of Galilei invariance on $1\hbar\omega$ transitions are seen for the square of the convection current form factor, too, which is presented in fig. 8. Again the normal description (2.47) yields a dramatic overestimation of the projected strength (2.50) at low momentum transfers, while here at momentum transfers above about 1.2 inverse Fm only small differences between the Tassie-Barker corrected normal and the projected result do remain. Finally, the squares of the spin current form factors (2.46) and (2.49) are presented in fig. 9. For this spin-flip transition the differences between the normal and the projected approach are again rather small at low momentum transfers and do remain small here even for higher momentum transfers.

Left to be considered are now the holes with an energy difference of $2\hbar\omega$ in ^{40}Ca . The results for the $1s-0s$ transition are given in the appendix.

For the scattering from the $0d$ to the $0s$ hole we get in the normal approximation

$$\begin{aligned}
F_{\text{ch, nor}}^{0s_{1/2 m}, 0d_{j' m'}}(Q^2) &= \delta_{m' m} f_{\tau}(Q^2) \\
&\cdot \exp\left\{-\frac{19}{78}\lambda^2\right\} \frac{1}{2} \sqrt{\frac{2j'+1}{30}} \lambda^2 [\delta_{j' \ 5/2} \pm \delta_{j' \ 3/2}], \quad (2.51)
\end{aligned}$$

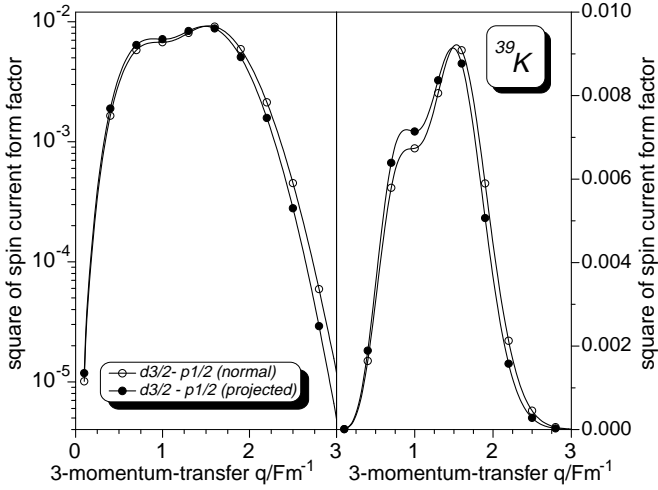


Fig. 9. Same as in fig. 7, but for the square of the spin current form factor.

while

$$F_{sc, \pm 1, \text{nor}}^{0s_{1/2m}, 0d_{j'm'}}(Q^2) = -\frac{G_M^\tau(Q^2)\hbar c}{Mc^2b} \exp\left\{-\frac{19}{78}\lambda^2\right\} \cdot \delta_{m' \pm 1/2} \delta_{m \mp 1/2} \frac{\sqrt{2j'+1}}{4\sqrt{15}} \lambda^3 [\delta_{j' 5/2} \pm \delta_{j' 3/2}] \quad (2.52)$$

and

$$F_{cc, \pm 1, \text{nor}}^{0s_{1/2m}, 0d_{j'm'}}(Q^2) = -\frac{f_\tau^{cc}(Q^2)\hbar c}{Mc^2b} \exp\left\{-\frac{19}{78}\lambda^2\right\} \frac{\lambda}{\sqrt{5}} \cdot \left[\delta_{j' 5/2} \left\{ \delta_{m' \pm 3/2} \delta_{m \pm 1/2} + \delta_{m' \pm 1/2} \delta_{m \mp 1/2} \frac{1}{\sqrt{2}} \right\} \pm \delta_{j' 3/2} \left\{ \delta_{m' \pm 3/2} \delta_{m \pm 1/2} \frac{1}{2} - \delta_{m' \pm 1/2} \delta_{m \mp 1/2} \frac{\sqrt{3}}{2} \right\} \right]. \quad (2.53)$$

With projection into the COM rest frame one obtains here

$$F_{ch, \text{pro}}^{0s_{1/2m}, 0d_{j'm'}}(Q^2) = -\delta_{m' m} \exp\left\{-\frac{19}{78}\lambda^2\right\} \frac{80}{117} \cdot \sqrt{\frac{10}{47}} \lambda^2 \sqrt{\frac{2j'+1}{10}} [\delta_{j' 5/2} \pm \delta_{j' 3/2}] \cdot \left[\frac{1}{80} \Phi_{40}(\lambda) - f_\tau(Q^2) \left\{ 1 - \frac{41}{3200}\lambda^2 + \frac{\lambda^4}{12800} \right\} \right], \quad (2.54)$$

while

$$F_{sc, \pm 1, \text{pro}}^{0s_{1/2m}, 0d_{j'm'}}(Q^2) = -\frac{G_M^\tau(Q^2)\hbar c}{Mc^2b} \cdot \exp\left\{-\frac{19}{78}\lambda^2\right\} \frac{80}{117} \sqrt{\frac{5}{47}} \lambda^3 \cdot \delta_{m' \pm 1/2} \delta_{m \mp 1/2} \sqrt{\frac{2j'+1}{10}} [\delta_{j' 5/2} \pm \delta_{j' 3/2}] \cdot \left\{ 1 - \frac{41}{3200}\lambda^2 + \frac{\lambda^4}{12800} \right\} \quad (2.55)$$

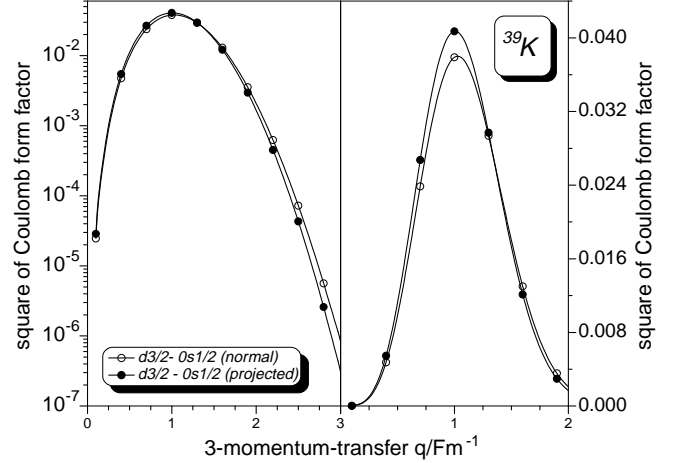


Fig. 10. The square of the Coulomb form factor in logarithmic (left side) and linear scale (right side) for the inelastic electron scattering from the $0d_{3/2}$ proton hole state in ^{40}O (*i.e.* the ground state of ^{39}K) to the $0s_{1/2}$ proton hole in the same nucleus (*i.e.* a $2\hbar\omega$ excited state of ^{39}K) are plotted *versus* the 3-momentum transfer. Again the results obtained with the normal approach are compared to those of the full Galilei-invariant description.

and

$$F_{cc, \pm 1, \text{pro}}^{0s_{1/2m}, 0d_{j'm'}}(Q^2) = \frac{\hbar c}{Mc^2b} \exp\left\{-\frac{19}{78}\lambda^2\right\} \frac{160}{39} \sqrt{\frac{2}{141}} \lambda \cdot \left[\delta_{j' 5/2} \left\{ \delta_{m' \pm 3/2} \delta_{m \pm 1/2} + \delta_{m' \pm 1/2} \delta_{m \mp 1/2} \frac{1}{\sqrt{2}} \right\} \pm \delta_{j' 3/2} \left\{ \delta_{m' \pm 3/2} \delta_{m \pm 1/2} \frac{1}{2} - \delta_{m' \pm 1/2} \delta_{m \mp 1/2} \frac{\sqrt{3}}{2} \right\} \right] \cdot \left[\frac{1}{80} \Phi_{40}^{cc}(\lambda) - f_\tau^{cc}(Q^2) \left\{ 1 - \frac{41}{3200}\lambda^2 + \frac{\lambda^4}{12800} \right\} \right]. \quad (2.56)$$

The results for the $0d_{3/2}$ - $0s_{1/2}$ transition in ^{39}K are summarized in figs. 10 to 12. Unlike the $1\hbar\omega$ transitions, this $2\hbar\omega$ transition is little affected by the full restoration of Galilei invariance. As already observed for the $0\hbar\omega$ transitions, also here only small differences are seen for the squares of the charge (fig. 10), the convection current (fig. 11) and the spin current (fig. 12) form factors.

2.3 Sum rules

For fixed 3-momentum transfer q and energy loss ω for the electron, the Coulomb scattering from the ground state $| \rangle$ of a considered nucleus is given (besides trivial kinematic factors) by the so-called longitudinal response function

$$R_L(q, \omega) \equiv \sum_m | \langle m | \hat{\rho} | \rangle |^2 \delta(\omega - E_m + E_0 - q^2/2MA), \quad (2.57)$$

where $|m\rangle$ denotes the excited states with excitation energy $E_m - E_0$ and the sum symbol means here a dis-

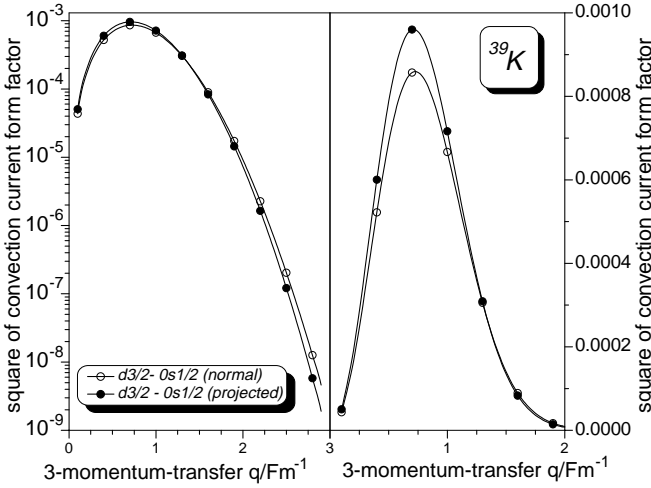


Fig. 11. Same as in fig. 10, but for the square of the convection current form factor.

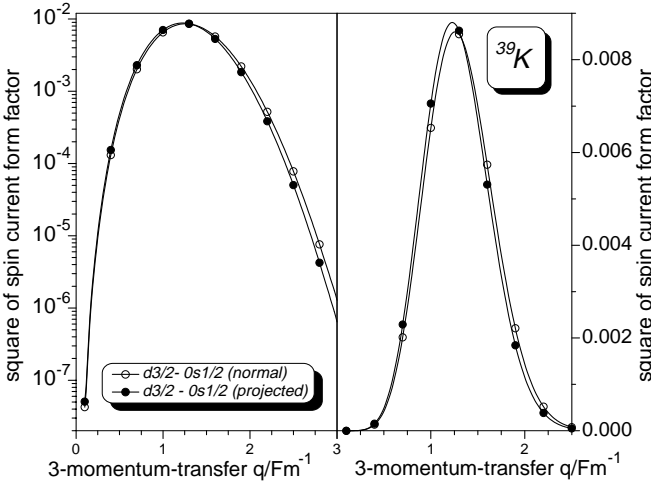


Fig. 12. Same as in fig. 10, but for the square of the spin current form factor.

crete sum over the bound and an integral over the continuum states. $q^2/2MA$ is the recoil energy of the considered system. Obviously, for a Galilei-invariant calculation, the invariant form (2.11) of the density operator as well as COM-projected ground and excited states have to be used.

Global properties of this response function can be obtained from its lowest moments ($n = 0, 1, 2, \dots$)

$$\Sigma_n^{\text{phys}}(q) \equiv \int_{\omega_{\min}}^{\omega_{\max}} d\omega \omega^n R_L(q, \omega), \quad (2.58)$$

where $\omega_{\min} \equiv q^2/2MA$ is given by the recoil energy and $\omega_{\max} \equiv q$ (here $\hbar = c = 1$). Equation (2.58) are the so-called “physical sum rules”.

If we assume point nucleons (setting the form factor (2.4) equal one for the protons and zero for the neutrons), then the operator $\hat{\rho}$ does not depend on the excitation energy of the system. If we, furthermore, assume that for

energy losses above ω_{\max} the response function is essentially vanishing, then we may integrate up to infinity and use the completeness of the final states (“closure approximation”). Under these assumptions we obtain from (2.58) the so-called “mathematical sum rules”. They play an important role in the analysis of correlations.

For Coulomb sum rule ($n = 0$) we obtain under these assumptions

$$\Sigma_0(q) = \langle |\hat{\rho}\hat{\rho}^\dagger| \rangle. \quad (2.59)$$

Note that here only the product of the density operator and its Hermitean conjugate enters. In this product the Gartenhaus-Schwartz operator out of (2.11) drops out. For the Coulomb sum rule it is therefore irrelevant, whether the invariant (2.11) or the usual form (2.3) of the charge density operator is used. The only difference between a Galilei-invariant and a usual calculation comes then from the use of the COM-projected instead of the normal ground state. If this ground state is a non-spurious oscillator state this projection drops out, and we obtain identical results with and without projection into the COM rest frame.

For the considered doubly even nuclei we hence obtain

$$\begin{aligned} \Sigma_0^{\text{pro}}(q) &\equiv \Sigma_0^{\text{nor}}(q) = Z + \exp\{-\lambda^2/2\} \\ &\cdot \frac{1}{\pi\sqrt{\pi}} \int d^3\vec{x} \exp\{-x^2\} \frac{1}{\pi\sqrt{\pi}} \int d^3\vec{z} \exp\{-z^2\} \\ &\cdot \left\{ 4y(\vec{x} - \vec{\lambda}/2, \vec{x} + \vec{\lambda}/2)y(\vec{z} + \vec{\lambda}/2, \vec{z} - \vec{\lambda}/2) \right. \\ &\quad \left. - 2y(\vec{x} - \vec{\lambda}/2, \vec{z} - \vec{\lambda}/2)y(\vec{z} + \vec{\lambda}/2, \vec{x} + \vec{\lambda}/2) \right\} = \\ &Z \left[1 + \exp\{-\lambda^2/2\} (Z - 1) \right. \\ &\cdot \left. \left\{ \begin{array}{ll} 1 & \text{for } ^4\text{He} \\ 1 - \frac{2\lambda^2}{7} + \frac{\lambda^4}{112} & \text{for } ^{16}\text{O} \\ 1 - \frac{10\lambda^2}{19} + \frac{13\lambda^4}{152} - \frac{9\lambda^6}{1520} + \frac{\lambda^8}{12160} & \text{for } ^{40}\text{Ca} \end{array} \right\} \right]. \quad (2.60) \end{aligned}$$

In the limit $q \rightarrow \infty$ these expressions yield the charge numbers Z . This is the limit of “quasi-elastic” scattering from the individual protons with no residual correlations. Deviations from this limit may hence be interpreted as “correlations”. In the limit $q \rightarrow 0$, however, the Coulomb sum rule is dominated by the elastic scattering and approaches Z^2 . In order to emphasize the correlations therefore usually the elastic scattering is subtracted from the Coulomb sum rule and the difference is furthermore divided by Z . One defines

$$\Sigma_0^{\text{inel}}(q) \equiv \frac{1}{Z} [\Sigma_0 - |F_{\text{ch}, A}(q)|^2], \quad (2.61)$$

where $F_{\text{ch}, A}(q)$ is given by eq. (2.22). This function starts at zero for low momentum transfer and approaches one for $q \rightarrow \infty$. If the Tassie-Barker factor is included in the normal calculation, then for non-spurious oscillator states $F_{\text{ch}, A}^{\text{nor}}(q) \equiv F_{\text{ch}, A}^{\text{pro}}(q)$, and consequently, for the simple A -nucleon ground states considered here, (2.61) gives again

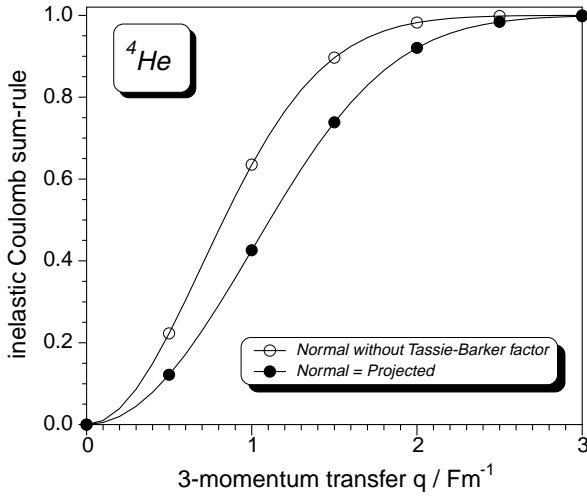


Fig. 13. The inelastic Coulomb sum rule for ${}^4\text{He}$ is displayed *versus* the 3-momentum transfer. Compared are the normal results without (open circles) and with (full circles) the Tassie-Barker factor. The latter approach is here identical to the full Galilei-invariant description.

identical results with or without projection into the COM rest frame. That the inclusion of the Tassie-Barker factor is rather essential can be seen from fig. 13, where for ${}^4\text{He}$ we have plotted (2.61) with

$$\Sigma_0^{\text{inel, nor}}(q) \equiv \Sigma_0^{\text{inel, pro}}(q) = \frac{1 + \exp\{-\lambda^2/2\} - 2\exp\{-3\lambda^2/8\}}{1 + \exp\{-\lambda^2/2\} - 2\exp\{-3\lambda^2/8\}} \quad (2.62)$$

and without

$$\Sigma_0^{\text{inel, no TB}}(q) = 1 - \exp\{-\lambda^2/2\} \quad (2.63)$$

this factor *versus* the 3-momentum transfer q . Since it includes the COM correlations, (2.62) approaches unity considerably slower than (2.63).

Holes within the last occupied shell of the considered doubly even systems are again non-spurious oscillator configurations and thus here again the projection into the COM rest frame yields the same result as the normal approach including the Tassie-Barker factor. More interesting are the hole states with excitation energy $\geq 1\hbar\omega$. They contain spurious admixtures and thus both, the elastic form factors as well as the Coulomb sum rule obtained with and without the projection into the COM rest frame become different. As an example we consider here the $0s$ proton-hole in ${}^{16}\text{O}$, *i.e.* an excited state in ${}^{15}\text{N}$. Though experimentally inaccessible, this example gives a hint what to expect in case that the ground state of a considered nucleus contains spurious admixtures. In the normal approach without the Tassie-Barker factor we obtain here

$$\Sigma_0^{\text{inel, no TB}}(q) = 1 + 6\exp\{-\lambda^2/2\} \left[1 - \frac{13\lambda^2}{42} + \frac{\lambda^4}{84} \right] - 7\exp\{-\lambda^2/2\} \left[1 - \frac{\lambda^2}{7} \right]^2, \quad (2.64)$$

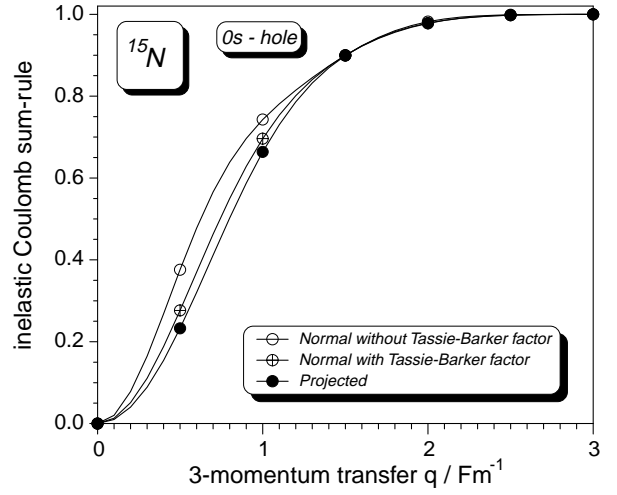


Fig. 14. Same as in fig. 13, but for the (theoretical) scattering from the $0s$ proton hole in ${}^{16}\text{O}$. Since this state has contaminations from the COM motion, Galilei-invariant and normal (Tassie-Barker corrected) description give here different results.

while with the Tassie-Barker correction one gets

$$\Sigma_0^{\text{inel, nor}}(q) = 1 + 6\exp\{-\lambda^2/2\} \left[1 - \frac{13\lambda^2}{42} + \frac{\lambda^4}{84} \right] - 7\exp\{-7\lambda^2/15\} \left[1 - \frac{\lambda^2}{7} \right]^2. \quad (2.65)$$

On the other hand, the Galilei-invariant result is here

$$\Sigma_0^{\text{inel, pro}}(q) = 1 + 6\exp\{-\lambda^2/2\} \left[1 - \frac{20\lambda^2}{63} + \frac{13\lambda^4}{1008} \right] - 7\exp\{-7\lambda^2/15\} \left[1 - \frac{44\lambda^2}{315} - \frac{\lambda^4}{5040} \right]^2. \quad (2.66)$$

Equations (2.64) to (2.66) are displayed *versus* the 3-momentum transfer q in fig. 14. It is clearly seen that here the simple inclusion of the Tassie-Barker factor alone is not sufficient.

Next, we discuss the first moment of the longitudinal response function, the so-called energy weighted sum rule. Dividing this moment by the Coulomb sum rule we get the most probable energy loss of the electron $\bar{\omega}$

$$\bar{\omega} \equiv \frac{\sum [E_m - E_0 + q^2/2MA] |\langle m | \hat{\rho} | \rangle|^2}{\Sigma_0}. \quad (2.67)$$

Using again point nucleons and the closure approximation we obtain immediately the well-known double-commutator expression

$$\bar{\omega} = \frac{1}{2} \frac{\langle [[\hat{\rho}^\dagger, [\hat{H}, \hat{\rho}]]] \rangle}{\Sigma_0} + \frac{q^2}{2MA}. \quad (2.68)$$

Using the point nucleon form of the normal charge density operator (2.3) and the usual operator of the kinetic

energy (2.2) (which is discussed in more detail in the next article of the present series of papers) one obtains without worrying about the COM

$$\begin{aligned}\bar{\omega}_{\text{nor}} &= \frac{q^2}{2M} \left[\frac{Z}{\Sigma_0^{\text{nor}}} + \frac{1}{A} \right] + \frac{1}{2} \frac{\langle \left| \left[\hat{\rho}^\dagger, [\hat{V}, \hat{\rho}] \right] \right| \rangle}{\Sigma_0^{\text{nor}}} \\ &\rightarrow \frac{q^2}{2M} \left[1 + \frac{1}{A} \right], \quad \text{for } q \rightarrow \infty. \quad (2.69)\end{aligned}$$

On the other hand the Galilei-invariant result is

$$\begin{aligned}\bar{\omega}_{\text{pro}} &\equiv \\ &\frac{1}{2} \frac{\langle \left| \left[\exp\{i\vec{q} \cdot \vec{R}_A\} \hat{\rho}^\dagger, [\hat{H}, \hat{\rho} \exp\{-i\vec{q} \cdot \vec{R}_A\}] \right] \hat{C}_A(0) \right| \rangle}{\langle |\hat{C}_A(0)| \rangle_{\Sigma_0^{\text{pro}}}} \\ &+ \frac{q^2}{2MA} = \frac{q^2}{2M} \frac{Z}{\Sigma_0^{\text{pro}}} \\ &+ \frac{1}{2} \frac{\langle \left| \left[\exp\{i\vec{q} \cdot \vec{R}_A\} \hat{\rho}^\dagger, [\hat{V}, \hat{\rho} \exp\{-i\vec{q} \cdot \vec{R}_A\}] \right] \hat{C}_A(0) \right| \rangle}{\langle |\hat{C}_A(0)| \rangle_{\Sigma_0^{\text{pro}}}} \\ &\rightarrow \frac{q^2}{2M}, \quad \text{for } q \rightarrow \infty, \quad (2.70)\end{aligned}$$

which is the expected result for quasi-elastic scattering. It should be stressed, however, that it is a little unfair to compare (2.70) with (2.69). As discussed in the next article of the present series of papers, for the normal approach at least the internal Hamiltonian $\hat{H} - \hat{P}_A^2/2MA$ should be used. Introducing furthermore the invariant form (2.11) of the charge density operator, we obtain at least in the large q limit the same result as with the full projection into the COM rest frame

$$\begin{aligned}\bar{\omega}_{\text{nor, corrected}} &\equiv \\ &\frac{1}{2} \frac{\langle \left| \left[\exp\{i\vec{q} \cdot \vec{R}_A\} \hat{\rho}^\dagger, \left[\hat{H} - \frac{\hat{P}_A^2}{2MA}, \hat{\rho} \exp\{-i\vec{q} \cdot \vec{R}_A\} \right] \right] \right| \rangle}{\Sigma_0^{\text{nor}}} \\ &+ \frac{q^2}{2MA} = \frac{q^2}{2M} \frac{Z}{\Sigma_0^{\text{nor}}} + \\ &\frac{1}{2} \frac{\langle \left| \left[\exp\{i\vec{q} \cdot \vec{R}_A\} \hat{\rho}^\dagger, [\hat{V}, \hat{\rho} \exp\{-i\vec{q} \cdot \vec{R}_A\}] \right] \right| \rangle}{\Sigma_0^{\text{nor}}} \\ &\rightarrow \frac{q^2}{2M}, \quad \text{for } q \rightarrow \infty. \quad (2.71)\end{aligned}$$

Finally, we come to the second moment of the longitudinal response function which is connected with its width. Here we obtain after a lengthy but straightforward calculation

in the normal approach

$$\begin{aligned}(\Delta\bar{\omega})_{\text{nor}}^2 &\equiv \left(\frac{\Sigma_2^{\text{nor}}}{\Sigma_0^{\text{nor}}} - \bar{\omega}_{\text{nor}}^2 \right) = \frac{q^2}{3MZ} \langle |\hat{T}| \rangle \\ &+ \frac{q^4}{4M^2} \frac{Z}{\Sigma_0^{\text{nor}}} \left[1 - \frac{Z}{\Sigma_0^{\text{nor}}} \right] \\ &+ \text{corrections } (\sim \exp\{-\lambda^2/2\}) \\ &+ \text{corrections } (\sim [\hat{V}, \hat{\rho}]) \\ &\rightarrow \frac{q^2}{3MZ} \langle |\hat{T}| \rangle, \quad \text{for } q \rightarrow \infty, \quad (2.72)\end{aligned}$$

while with projection into the COM rest frame one gets

$$\begin{aligned}(\Delta\bar{\omega})_{\text{pro}}^2 &\equiv \left(\frac{\Sigma_2^{\text{pro}}}{\Sigma_0^{\text{pro}}} - \bar{\omega}_{\text{pro}}^2 \right) = \frac{q^2}{3MZ} \frac{\langle |\hat{T} \hat{C}_A(0)| \rangle}{\langle |\hat{C}_A(0)| \rangle} \\ &+ \frac{q^4}{4M^2} \left[1 - \frac{Z}{\Sigma_0^{\text{nor}}} \right] \left[\frac{A+2}{A} + \frac{Z}{\Sigma_0^{\text{pro}}} \right] \\ &+ \text{corrections } (\sim \exp\{-\lambda^2/2\}) \\ &+ \text{corrections } (\sim [\hat{V}, \hat{\rho} \exp\{-i\vec{q} \cdot \vec{R}_A\}]) \\ &\rightarrow \frac{q^2}{3MZ} \frac{\langle |\hat{T} \hat{C}_A(0)| \rangle}{\langle |\hat{C}_A(0)| \rangle}, \quad \text{for } q \rightarrow \infty. \quad (2.73)\end{aligned}$$

As expected, the width of the longitudinal response function is given essentially by the so-called ‘‘Fermi motion’’. It is proportional to the square root of the average kinetic energy per proton in the direction of the 3-momentum transfer. The COM projected value for this quantity (see next article) is smaller than the unprojected one. This difference, however, goes again with $1/A$.

3 Conclusions

In the present article the influence of the restoration of Galilei invariance on the electromagnetic properties of simple bound states has been investigated. For this purpose the form factors for elastic electron scattering from the oscillator ground states of ${}^4\text{He}$, ${}^{16}\text{O}$ and ${}^{40}\text{Ca}$ as well as for the transitions between the various one-hole states with respect to these reference configurations have been calculated with projection into the COM rest frame. The results have then been compared to those obtained without projection but correcting for the COM motion in the usual way by introducing the Tassie-Barker factor.

The results can be summarized as follows. Only small effects on top of the Tassie-Barker correction are seen for the $0\hbar\omega$ and $2\hbar\omega$ transitions. Here the usual prescription seems to work well. However, we have to take into account that only simple oscillator configurations were considered. If both initial and final configuration are non-spurious, then the Tassie-Barker correction is identical to the COM projected result. If more general wave functions are considered (*e.g.*, Hartree-Fock or Woods-Saxon ones) this picture would change. In fact, in this case considerable effects of the projection on top of the Tassie-Barker correction are

already seen in the elastic electron scattering from doubly even nuclei [4, 5].

On the other hand, drastic differences between the Tassie-Barker corrected normal approach and the full COM projected description are obtained for the $1\hbar\omega$ transitions. As far as the charge and the convection current are concerned the normal approach overestimates the COM projected strength at low momentum transfer dramatically, while at higher momentum transfer the situation is reversed. On the other hand, only small effects are seen for the spin current. The reason is that the latter is connected with a spin-flip which cannot be induced by the COM motion. The strong effects of the restoration of Galilei invariance are of the same size in ^{15}N and in ^{39}K and thus clearly not a $1/A$ effect.

That the $1\hbar\omega$ transitions are strongly affected was to be expected from the electric dipole transitions with real photons. Here usually an effective dipole operator is introduced to eliminate the spurious isoscalar excitations in which protons and neutrons move in phase and thus produce only a “shift” of the total nucleus. It should be stressed, however, that this well-known approach does only work for real photons. If, as in electron scattering the whole momentum dependence is tested, then the spurious admixtures have to be eliminated by projection as done in the present paper.

In the second part of the present paper then the (mathematical) Coulomb sum rules and their first and second moments were investigated for the three considered doubly even nuclei. Since the oscillator ground states of these nuclei are non-spurious, and since the Gartenhaus-Schwartz modification of the charge density drops out, the normal and COM projected results for the Coulomb sum rules are identical. Some care, however, is necessary if as usual instead of the Coulomb sum rules their “inelastic” versions are considered. Here the form factor for the elastic scattering enters which definitely has to be corrected by the Tassie-Barker factor in order to obtain reasonable results. In case that the target state contains spurious admixtures, the Tassie-Barker correction is not sufficient. This has been demonstrated for the hypothetical scattering from a $0s$ -proton-hole in ^{16}O .

For the first and second moments of the Coulomb sum rule the restoration of Galilei invariance finally gives a clear $1/A$ effect. So, for the most probable energy loss of the electron the COM projected approach predicts (in the large q limit) the expected quasi-elastic result while in the normal approach a shift to higher-energy losses by a factor $(1 + 1/A)$ is obtained. The width of the quasi-elastic peak (to be obtained from the second moment) is essentially given by the expectation value of the kinetic energy in the target state (Fermi motion). In the COM projected approach here the Galilei-invariant ground state enters which produces a smaller kinetic energy and hence a smaller width. This effect, however, is proportional to $1/A$, too.

Appendix A.

In this appendix we complete the results for the form factors out of subsect. 2.2. We start with the $0\hbar\omega$ transitions between “non-spurious” oscillator states. For the $0s$ holes in ^4He , we obtain

$$F_{\text{ch, nor}}^{0s_{1/2m}, 0s_{1/2m'}}(Q^2) = F_{\text{ch, pro}}^{0s_{1/2m}, 0s_{1/2m'}}(Q^2) = \exp\left\{-\frac{1}{6}\lambda^2\right\} \delta_{m'm} [2\Phi_4(\lambda) - f_\tau(Q^2)] \quad (\text{A.1})$$

and

$$F_{\text{sc}, \pm 1, \text{nor}}^{0s_{1/2m}, 0s_{1/2m'}}(Q^2) = F_{\text{sc}, \pm 1, \text{pro}}^{0s_{1/2m}, 0s_{1/2m'}}(Q^2) = \exp\left\{-\frac{1}{6}\lambda^2\right\} \delta_{m' \pm 1/2} \delta_{m \mp 1/2} \frac{\lambda}{\sqrt{2}} \frac{G_M^\tau(Q^2)\hbar c}{Mc^2b}, \quad (\text{A.2})$$

while the convection current does not contribute to the scattering between s holes. Note, that we consider hole states. That is why the matrix elements get a phase of $(-)^{j-j'}$ for the charge density and $(-)^{j+j'}$ for the currents. Furthermore this is the reason why the subscript at the current form factor is $\eta = \pm 1 = m' - m$ instead of the other way round.

For the scattering between the $0p$ holes in ^{16}O , we get

$$F_{\text{ch, nor}}^{0p_{jm}, 0p_{j'm'}}(Q^2) = F_{\text{ch, pro}}^{0p_{jm}, 0p_{j'm'}}(Q^2) = \delta_{m'm} \exp\left\{-\frac{7}{30}\lambda^2\right\} \cdot \left[\delta_{j'j} \left\{ 8\Phi_{16}(\lambda) - f_\tau(Q^2) \left[1 - \frac{1}{6}\lambda^2 \right] \right\} + f_\tau(Q^2) \frac{1}{6}\lambda^2 (-)^{m-1/2} \sqrt{(2j+1)(2j'+1)} \cdot (jj'2|m-m0)(jj'2|1/2-1/20) \right], \quad (\text{A.3})$$

where we have isolated the scalar (“monopole”) part of the density explicitly, since we shall need it in the next article of the present series of papers. For the spin current, we get here

$$F_{\text{sc}, \pm 1, \text{nor}}^{0p_{jm}, 0p_{j'm'}}(Q^2) = F_{\text{sc}, \pm 1, \text{pro}}^{0p_{jm}, 0p_{j'm'}}(Q^2) = \frac{G_M^\tau(Q^2)\hbar c}{Mc^2b} \exp\left\{-\frac{7}{30}\lambda^2\right\} \frac{\lambda}{\sqrt{2}} \cdot \left[\delta_{j'3/2} \delta_{j'3/2} \left\{ [\delta_{m' \pm 3/2} \delta_{m \pm 1/2} + \delta_{m' \mp 1/2} \delta_{m \mp 3/2}] \frac{1}{\sqrt{3}} + \delta_{m' \pm 1/2} \delta_{m \mp 1/2} \frac{2}{3} \left[1 - \frac{1}{2}\lambda^2 \right] \right\} - \delta_{j'1/2} \delta_{j'1/2} \left\{ \delta_{m' \pm 1/2} \delta_{m \mp 1/2} \frac{1}{3} \left[1 - \frac{1}{2}\lambda^2 \right] \right\} \mp \delta_{j'1/2} \delta_{j'3/2} \left\{ \delta_{m' \pm 3/2} \delta_{m \pm 1/2} \sqrt{\frac{2}{3}} \right\} \right]$$

$$\begin{aligned}
& + \delta_{m'\pm 1/2} \delta_{m\mp 1/2} \frac{\sqrt{2}}{3} \left[1 - \frac{1}{2} \lambda^2 \right] \Big\} \\
& \pm \delta_{j\ 3/2} \delta_{j'\ 1/2} \left\{ \delta_{m'\mp 1/2} \delta_{m\mp 3/2} \sqrt{\frac{2}{3}} \right. \\
& \left. + \delta_{m'\pm 1/2} \delta_{m\mp 1/2} \frac{\sqrt{2}}{3} \left[1 - \frac{1}{2} \lambda^2 \right] \right\} \quad (A.4) \\
& \cdot \left[\delta_{j'j} \left\{ 20 \Phi_{40}(\lambda) - f_\tau(Q^2) \left\{ 1 - \frac{1}{3} \lambda^2 + \frac{1}{60} \lambda^4 \right\} \right\} \right. \\
& \left. - f_\tau(Q^2) \sum_{L=2,4} (-)^{m-1/2} \sqrt{(2j+1)(2j'+1)} \right. \\
& \left. \cdot (jj'L|m-m0)(jj'L|1/2-1/20) \rho_L^{0d0d} \right], \quad (A.8)
\end{aligned}$$

and the convection current yields

$$\begin{aligned}
& F_{cc,\pm 1, \text{nor}}^{0pjm, 0p_j'm'}(Q^2) = F_{cc,\pm 1, \text{pro}}^{0pjm, 0p_j'm'}(Q^2) = \\
& \frac{f_\tau^{cc}(Q^2) \hbar c}{Mc^2 b} \exp \left\{ -\frac{7}{30} \lambda^2 \right\} \frac{\lambda}{2} \\
& \cdot \left[\delta_{j\ 3/2} \delta_{j'\ 3/2} \left\{ [\delta_{m'\pm 3/2} \delta_{m\pm 1/2} + \delta_{m'\mp 1/2} \delta_{m\mp 3/2}] \right. \right. \\
& \left. \left. \cdot \sqrt{\frac{2}{3}} + \delta_{m'\pm 1/2} \delta_{m\mp 1/2} \frac{2\sqrt{2}}{3} \right\} \right. \\
& + \delta_{j\ 1/2} \delta_{j'\ 1/2} \left\{ \delta_{m'\pm 1/2} \delta_{m\mp 1/2} \frac{2\sqrt{2}}{3} \right\} \\
& \pm \delta_{j\ 1/2} \delta_{j'\ 3/2} \left\{ \delta_{m'\pm 3/2} \delta_{m\pm 1/2} \frac{1}{\sqrt{3}} + \delta_{m'\pm 1/2} \delta_{m\mp 1/2} \frac{1}{3} \right\} \\
& \mp \delta_{j\ 3/2} \delta_{j'\ 1/2} \left\{ \delta_{m'\mp 1/2} \delta_{m\mp 3/2} \frac{1}{\sqrt{3}} + \delta_{m'\pm 1/2} \delta_{m\mp 1/2} \frac{1}{3} \right\} \Big]. \quad (A.5)
\end{aligned}$$

For the scattering between the $1s$ holes in ^{40}Ca , one gets

$$\begin{aligned}
& F_{\text{ch, nor}}^{1s_{1/2m}, 1s_{1/2m'}}(Q^2) = F_{\text{ch, pro}}^{1s_{1/2m}, 1s_{1/2m'}}(Q^2) = \\
& \delta_{m'm} \exp \left\{ -\frac{19}{78} \lambda^2 \right\} \\
& \cdot \left[20 \Phi_{40}(\lambda) - f_\tau(Q^2) \left\{ 1 - \frac{1}{3} \lambda^2 + \frac{1}{24} \lambda^4 \right\} \right] \quad (A.6)
\end{aligned}$$

and

$$\begin{aligned}
& F_{\text{sc}, \pm 1, \text{nor}}^{1s_{1/2m}, 1s_{1/2m'}}(Q^2) = F_{\text{sc}, \pm 1, \text{pro}}^{1s_{1/2m}, 1s_{1/2m'}}(Q^2) = \\
& \frac{G_M^\tau(Q^2) \hbar c}{Mc^2 b} \exp \left\{ -\frac{19}{78} \lambda^2 \right\} \\
& \cdot \delta_{m'\pm 1/2} \delta_{m\mp 1/2} \frac{\lambda}{\sqrt{2}} \left\{ 1 - \frac{1}{3} \lambda^2 + \frac{1}{24} \lambda^4 \right\}. \quad (A.7)
\end{aligned}$$

Furthermore, for the scattering between the $0d$ holes in ^{40}Ca , the results are

$$\begin{aligned}
& F_{\text{ch, nor}}^{0d_{jm}, 0d_{j'm'}}(Q^2) = \\
& F_{\text{ch, pro}}^{0d_{jm}, 0d_{j'm'}}(Q^2) = \delta_{m'm} \exp \left\{ -\frac{19}{78} \lambda^2 \right\} \\
& \cdot \left[\delta_{j'j} \left\{ 20 \Phi_{40}(\lambda) - f_\tau(Q^2) \left\{ 1 - \frac{1}{3} \lambda^2 + \frac{1}{60} \lambda^4 \right\} \right\} \right. \\
& \left. - f_\tau(Q^2) \sum_{L=2,4} (-)^{m-1/2} \sqrt{(2j+1)(2j'+1)} \right. \\
& \left. \cdot (jj'L|m-m0)(jj'L|1/2-1/20) \rho_L^{0d0d} \right], \quad (A.8)
\end{aligned}$$

where we have again isolated the monopole part. By definition

$$\rho_2^{0d0d} \equiv -\frac{7}{30} \lambda^2 \left\{ 1 - \frac{1}{14} \lambda^2 \right\}, \quad \text{and} \quad \rho_4^{0d0d} \equiv \frac{1}{60} \lambda^4. \quad (A.9)$$

Furthermore, here

$$\begin{aligned}
& F_{\text{sc}, \pm 1, \text{nor}}^{0d_{jm}, 0d_{j'm'}}(Q^2) = F_{\text{sc}, \pm 1, \text{pro}}^{0d_{jm}, 0d_{j'm'}}(Q^2) = \\
& \frac{G_M^\tau(Q^2) \hbar c}{Mc^2 b} \exp \left\{ -\frac{19}{78} \lambda^2 \right\} \frac{\lambda}{\sqrt{2}} \\
& \cdot \left[\delta_{j\ 5/2} \delta_{j'\ 5/2} \left\{ [\delta_{m'\pm 5/2} \delta_{m\pm 3/2} + \delta_{m'\mp 3/2} \delta_{m\mp 5/2}] \right. \right. \\
& \left. \left. \cdot \frac{1}{\sqrt{5}} + [\delta_{m'\pm 3/2} \delta_{m\pm 1/2} + \delta_{m'\mp 1/2} \delta_{m\mp 3/2}] \frac{2\sqrt{2}}{5} \right\} \right. \\
& \left. \cdot \left[1 - \frac{1}{2} \lambda^2 \right] + \delta_{m'\pm 1/2} \delta_{m\mp 1/2} \frac{3}{5} \left[1 - \frac{2}{3} \lambda^2 + \frac{1}{12} \lambda^4 \right] \right\} \\
& - \delta_{j\ 3/2} \delta_{j'\ 3/2} \left\{ [\delta_{m'\pm 3/2} \delta_{m\pm 1/2} + \delta_{m'\mp 1/2} \delta_{m\mp 3/2}] \right. \\
& \left. \cdot \frac{\sqrt{3}}{5} \left[1 - \frac{1}{2} \lambda^2 \right] + \delta_{m'\pm 1/2} \delta_{m\mp 1/2} \right. \\
& \left. \cdot \frac{2}{5} \left[1 - \frac{2}{3} \lambda^2 + \frac{1}{12} \lambda^4 \right] \right\} \pm \delta_{j\ 5/2} \delta_{j'\ 3/2} \\
& \cdot \left\{ \delta_{m'\mp 3/2} \delta_{m\mp 5/2} \frac{2}{\sqrt{5}} + \delta_{m'\pm 1/2} \delta_{m\mp 1/2} \right. \\
& \left. \cdot \frac{\sqrt{6}}{5} \left[1 - \frac{2}{3} \lambda^2 + \frac{1}{12} \lambda^4 \right] + [\delta_{m'\pm 3/2} \delta_{m\pm 1/2}] \frac{\sqrt{2}}{5} \right. \\
& \left. + \delta_{m'\mp 1/2} \delta_{m\mp 3/2} \frac{2\sqrt{3}}{5} \right] \left[1 - \frac{1}{2} \lambda^2 \right] \Big\} \\
& \mp \delta_{j\ 3/2} \delta_{j'\ 5/2} \left\{ \delta_{m'\pm 5/2} \delta_{m\pm 3/2} \frac{2}{\sqrt{5}} \right. \\
& + \delta_{m'\pm 1/2} \delta_{m\mp 1/2} \frac{\sqrt{6}}{5} \left[1 - \frac{2}{3} \lambda^2 + \frac{1}{12} \lambda^4 \right] \\
& \left. + [\delta_{m'\pm 3/2} \delta_{m\pm 1/2}] \frac{2\sqrt{3}}{5} \right. \\
& \left. + \delta_{m'\mp 1/2} \delta_{m\mp 3/2} \frac{\sqrt{2}}{5} \right] \left[1 - \frac{1}{2} \lambda^2 \right] \Big\} \quad (A.10)
\end{aligned}$$

and

$$\begin{aligned}
F_{cc, \pm 1, \text{nor}}^{0d_{j m}, 0d_{j' m'}}(Q^2) &= F_{cc, \pm 1, \text{pro}}^{0d_{j m}, 0d_{j' m'}}(Q^2) = \\
&= -\frac{f_{\tau}^{\text{cc}}(Q^2)\hbar c}{Mc^2b} \exp\left\{-\frac{19}{78}\lambda^2\right\} \frac{\lambda}{\sqrt{2}} \\
&\cdot \left[\delta_{j 5/2} \delta_{j' 5/2} \left\{ \left[\delta_{m' \pm 5/2} \delta_{m \pm 3/2} + \delta_{m' \mp 3/2} \delta_{m \mp 5/2} \right] \right. \right. \\
&\cdot \frac{2}{\sqrt{5}} + \left. \left[\delta_{m' \pm 3/2} \delta_{m \pm 1/2} + \delta_{m' \mp 1/2} \delta_{m \mp 3/2} \right] \right. \\
&\cdot \left. \left. \frac{4\sqrt{2}}{5} \left[1 - \frac{1}{8}\lambda^2 \right] + \delta_{m' \pm 1/2} \delta_{m \mp 1/2} \frac{6}{5} \left[1 - \frac{1}{6}\lambda^2 \right] \right\} \right. \\
&+ \delta_{j 3/2} \delta_{j' 3/2} \left\{ \left[\delta_{m' \pm 3/2} \delta_{m \pm 1/2} + \delta_{m' \mp 1/2} \delta_{m \mp 3/2} \right] \right. \\
&\cdot \left. \left. \frac{3\sqrt{3}}{5} \left[1 - \frac{1}{18}\lambda^2 \right] + \delta_{m' \pm 1/2} \delta_{m \mp 1/2} \frac{6}{5} \left[1 - \frac{1}{6}\lambda^2 \right] \right\} \right. \\
&\mp \delta_{j 5/2} \delta_{j' 3/2} \left\{ \delta_{m' \mp 3/2} \delta_{m \mp 5/2} \frac{1}{\sqrt{5}} \right. \\
&+ \delta_{m' \pm 1/2} \delta_{m \mp 1/2} \frac{\sqrt{3}}{5\sqrt{2}} \left[1 - \frac{1}{6}\lambda^2 \right] \\
&+ \delta_{m' \pm 3/2} \delta_{m \pm 1/2} \frac{1}{5\sqrt{2}} \left[1 + \frac{1}{2}\lambda^2 \right] \\
&+ \left. \left. \delta_{m' \mp 1/2} \delta_{m \mp 3/2} \frac{\sqrt{3}}{5} \left[1 - \frac{1}{3}\lambda^2 \right] \right\} \right. \\
&\pm \delta_{j 3/2} \delta_{j' 5/2} \left\{ \delta_{m' \pm 5/2} \delta_{m \pm 3/2} \frac{1}{\sqrt{5}} \right. \\
&+ \delta_{m' \pm 1/2} \delta_{m \mp 1/2} \frac{\sqrt{3}}{5\sqrt{2}} \left[1 - \frac{1}{6}\lambda^2 \right] \\
&+ \delta_{m' \pm 3/2} \delta_{m \pm 1/2} \frac{\sqrt{3}}{5} \left[1 - \frac{1}{3}\lambda^2 \right] \\
&+ \left. \left. \delta_{m' \mp 1/2} \delta_{m \mp 3/2} \frac{1}{5\sqrt{2}} \left[1 + \frac{1}{2}\lambda^2 \right] \right\} \right]. \quad (\text{A.11})
\end{aligned}$$

Finally, for the matrix elements between the $1s$ and $0d$ holes in ^{40}Ca , we obtain

$$\begin{aligned}
F_{\text{ch}, \text{nor}}^{1s_{1/2 m}, 0d_{j' m'}}(Q^2) &= F_{\text{ch}, \text{pro}}^{1s_{1/2 m}, 0d_{j' m'}}(Q^2) = \\
&= -f_{\tau}(Q^2) \exp\left\{-\frac{19}{78}\lambda^2\right\} \delta_{m' m} \frac{1}{3} \sqrt{\frac{2j'+1}{5}} \\
&\cdot \left[\delta_{j' 5/2} + (-)^{1/2-m} \delta_{j' 3/2} \lambda^2 \left\{ 1 - \frac{1}{8}\lambda^2 \right\} \right], \quad (\text{A.12})
\end{aligned}$$

while

$$\begin{aligned}
F_{\text{sc}, \pm 1, \text{nor}}^{1s_{1/2 m}, 0d_{j' m'}}(Q^2) &= F_{\text{sc}, \pm 1, \text{pro}}^{1s_{1/2 m}, 0d_{j' m'}}(Q^2) = \\
&= \frac{G_M^{\tau}(Q^2)\hbar c}{Mc^2b} \exp\left\{-\frac{19}{78}\lambda^2\right\} \delta_{m' \pm 1/2} \delta_{m \mp 1/2} \frac{1}{3} \sqrt{\frac{2j'+1}{10}} \\
&\cdot \left[\delta_{j' 5/2} + (-)^{1/2-m} \delta_{j' 3/2} \lambda^3 \left\{ 1 - \frac{1}{8}\lambda^2 \right\} \right] \quad (\text{A.13})
\end{aligned}$$

and

$$\begin{aligned}
F_{\text{cc}, \pm 1, \text{nor}}^{1s_{1/2 m}, 0d_{j' m'}}(Q^2) &= F_{\text{cc}, \pm 1, \text{pro}}^{1s_{1/2 m}, 0d_{j' m'}}(Q^2) = \\
&= -\frac{f_{\tau}^{\text{cc}}(Q^2)\hbar c}{Mc^2b} \exp\left\{-\frac{19}{78}\lambda^2\right\} \frac{\lambda^3}{4\sqrt{30}} \\
&\cdot \left[\delta_{j' 5/2} \left\{ \delta_{m' \pm 3/2} \delta_{m \pm 1/2} 2 + \delta_{m' \pm 1/2} \delta_{m \mp 1/2} \sqrt{2} \right\} \right. \\
&\pm \delta_{j' 3/2} \left\{ \delta_{m' \pm 3/2} \delta_{m \pm 1/2} + \delta_{m' \pm 1/2} \delta_{m \mp 1/2} \sqrt{3} \right\} \left. \right]. \quad (\text{A.14})
\end{aligned}$$

Next, we list the results for those $1\hbar\omega$ transitions in ^{40}Ca which have not been presented in subsect. 2.2. For the $0p$ to $0s$ transition, we obtain here in the normal case

$$\begin{aligned}
F_{\text{ch}, \text{nor}}^{0s_{1/2 m}, 0p_{j' m'}}(Q^2) &= \delta_{m' m} f_{\tau}(Q^2) \exp\left\{-\frac{19}{78}\lambda^2\right\} \\
&\cdot \frac{i\lambda}{2} \sqrt{\frac{2j'+1}{3}} \left[\delta_{j' 3/2} + (-)^{1/2-m} \delta_{j' 1/2} \right], \quad (\text{A.15})
\end{aligned}$$

while

$$\begin{aligned}
F_{\text{sc}, \pm 1, \text{nor}}^{0s_{1/2 m}, 0p_{j' m'}}(Q^2) &= \\
&= -\delta_{m' \pm 1/2} \delta_{m \mp 1/2} \frac{G_M^{\tau}(Q^2)\hbar c}{Mc^2b} \exp\left\{-\frac{19}{78}\lambda^2\right\} \\
&\cdot \frac{i\lambda^2}{2\sqrt{2}} \sqrt{\frac{2j'+1}{3}} \left[\delta_{j' 3/2} \pm \delta_{j' 1/2} \right] \quad (\text{A.16})
\end{aligned}$$

and

$$\begin{aligned}
F_{\text{cc}, \pm 1, \text{nor}}^{0s_{1/2 m}, 0p_{j' m'}}(Q^2) &= \\
&= -\frac{f_{\tau}^{\text{cc}}(Q^2)\hbar c}{Mc^2b} \exp\left\{-\frac{19}{78}\lambda^2\right\} \frac{i}{\sqrt{2}} \\
&\cdot \left[\delta_{j' 3/2} \left\{ \delta_{m' \pm 3/2} \delta_{m \pm 1/2} + \delta_{m' \pm 1/2} \delta_{m \mp 1/2} \frac{1}{\sqrt{3}} \right\} \right. \\
&\mp \left. \delta_{j' 3/2} \delta_{m' \pm 1/2} \delta_{m \mp 1/2} \sqrt{\frac{2}{3}} \right] \quad (\text{A.17})
\end{aligned}$$

Note that again except for the different exponential these results are identical to (2.39) to (2.41) obtained for ^{16}O . With projection into the COM rest frame, however,

this does not hold anymore. We obtain

$$\begin{aligned}
F_{\text{ch, pro}}^{0\bar{s}_{1/2m}, 0p_{j'm'}}(Q^2) &= -\delta_{m'm} \exp\left\{-\frac{19}{78}\lambda^2\right\} \\
&\cdot \frac{i\lambda}{2} \sqrt{\frac{5600}{5499}} \sqrt{\frac{2j'+1}{3}} \left[\delta_{j'3/2} + (-)^{1/2-m}\delta_{j'1/2}\right] \\
&\cdot \left[\frac{1}{2}\Phi_{40}(\lambda) - f_\tau(Q^2) \left[1 - \frac{281}{21840}\lambda^2\right.\right. \\
&\left.\left. + \frac{43}{436800}\lambda^4 - \frac{1}{873600}\lambda^6\right]\right], \quad (\text{A.18})
\end{aligned}$$

while

$$\begin{aligned}
F_{\text{sc}, \pm 1, \text{pro}}^{0\bar{s}_{1/2m}, 0p_{j'm'}}(Q^2) &= -\delta_{m' \pm 1/2} \delta_{m \mp 1/2} \\
&\cdot \frac{G_M^\tau(Q^2)\hbar c}{Mc^2b} \exp\left\{-\frac{19}{78}\lambda^2\right\} \\
&\cdot \frac{i\lambda^2}{2\sqrt{2}} \sqrt{\frac{5600}{5499}} \sqrt{\frac{2j'+1}{3}} \left[\delta_{j'3/2} \pm \delta_{j'1/2}\right] \\
&\cdot \left\{1 - \frac{281}{21840}\lambda^2 + \frac{43}{436800}\lambda^4 - \frac{1}{873600}\lambda^6\right\} \quad (\text{A.19})
\end{aligned}$$

and

$$\begin{aligned}
F_{\text{cc}, \pm 1, \text{pro}}^{0\bar{s}_{1/2m}, 0p_{j'm'}}(Q^2) &= \frac{\hbar c}{Mc^2b} \exp\left\{-\frac{19}{78}\lambda^2\right\} \frac{i}{\sqrt{2}} \sqrt{\frac{5600}{5499}} \\
&\cdot \left[\delta_{j'3/2} \left\{\delta_{m' \pm 3/2} \delta_{m \pm 1/2} + \delta_{m' \pm 1/2} \delta_{m \mp 1/2} \frac{1}{\sqrt{3}}\right\}\right. \\
&\left. \mp \delta_{j'3/2} \delta_{m' \pm 1/2} \delta_{m \mp 1/2} \sqrt{\frac{2}{3}}\right] \\
&\cdot \left[\frac{1}{2}\Phi_{40}^{\text{cc}}(\lambda) - f_\tau^{\text{cc}}(Q^2) \left\{1 - \frac{281}{21840}\lambda^2\right.\right. \\
&\left.\left. + \frac{43}{436800}\lambda^4 - \frac{1}{873600}\lambda^6\right\}\right]. \quad (\text{A.20})
\end{aligned}$$

The structure of these results is rather similar to that obtained for the $0p$ - $0s$ form factors in the $A = 15$ system. Again there occurs an ‘‘elastic term’’ in the projected charge and convection current form factors which is absent for the spin-flip transition. The effects are similar to those displayed in fig. 4 to 6 and will hence not be shown in the present article.

In ^{40}Ca we can furthermore consider the $1s$ - $0p$ form factors. Here, we obtain in the normal approximation

$$\begin{aligned}
F_{\text{ch, nor}}^{0p_{jm}, 1s_{1/2m'}}(Q^2) &= -\delta_{m'm} f_\tau(Q^2) \exp\left\{-\frac{19}{78}\lambda^2\right\} \\
&\cdot \frac{i\lambda}{3\sqrt{2}} \sqrt{2j'+1} \left[\delta_{j'3/2} + (-)^{1/2-m}\delta_{j'1/2}\right] \left\{1 - \frac{1}{4}\lambda^2\right\}, \quad (\text{A.21})
\end{aligned}$$

while

$$\begin{aligned}
F_{\text{sc}, \pm 1, \text{nor}}^{0p_{jm}, 1s_{1/2m'}}(Q^2) &= \delta_{m' \pm 1/2} \delta_{m \mp 1/2} \\
&\cdot \frac{G_M^\tau(Q^2)\hbar c}{Mc^2b} \exp\left\{-\frac{19}{78}\lambda^2\right\} \\
&\cdot \frac{i\lambda^2}{6} \sqrt{2j'+1} \left[\delta_{j'3/2} \pm \delta_{j'1/2}\right] \left\{1 - \frac{1}{4}\lambda^2\right\} \quad (\text{A.22})
\end{aligned}$$

and

$$\begin{aligned}
F_{\text{cc}, \pm 1, \text{nor}}^{0p_{jm}, 1s_{1/2m'}}(Q^2) &= \\
&-\frac{f_\tau^{\text{cc}}(Q^2)\hbar c}{Mc^2b} \exp\left\{-\frac{19}{78}\lambda^2\right\} \frac{i}{\sqrt{6}} \left\{1 + \frac{1}{4}\lambda^2\right\} \\
&\cdot \left[\delta_{j'3/2} \left\{\delta_{m' \pm 3/2} \delta_{m \pm 1/2} + \delta_{m' \pm 1/2} \delta_{m \mp 1/2} \frac{1}{\sqrt{3}}\right\}\right. \\
&\left. \mp \delta_{j'3/2} \delta_{m' \pm 1/2} \delta_{m \mp 1/2} \sqrt{\frac{2}{3}}\right] \quad (\text{A.23})
\end{aligned}$$

With projection into the COM rest frame, we obtain, on the other hand,

$$\begin{aligned}
F_{\text{ch, pro}}^{0p_{jm}, 1s_{1/2m'}}(Q^2) &= \\
&\delta_{m'm} \exp\left\{-\frac{19}{78}\lambda^2\right\} \frac{i\lambda}{3\sqrt{2}} \frac{40}{\sqrt{1365}} \sqrt{2j'+1} \\
&\cdot \left[\delta_{j'3/2} + (-)^{1/2-m}\delta_{j'1/2}\right] \left[\frac{1}{2}\Phi_{40}(\lambda)\right. \\
&\left. - f_\tau(Q^2) \frac{40}{\sqrt{1365}} \left\{1 - \frac{43}{160}\lambda^2 + \frac{1}{320}\lambda^4\right\}\right], \quad (\text{A.24})
\end{aligned}$$

while

$$\begin{aligned}
F_{\text{sc}, \pm 1, \text{pro}}^{0p_{jm}, 1s_{1/2m'}}(Q^2) &= \\
&\delta_{m' \pm 1/2} \delta_{m \mp 1/2} \frac{G_M^\tau(Q^2)\hbar c}{Mc^2b} \exp\left\{-\frac{19}{78}\lambda^2\right\} \\
&\cdot \frac{i\lambda^2}{6} \frac{40}{\sqrt{1365}} \sqrt{2j'+1} \left[\delta_{j'3/2} \pm \delta_{j'1/2}\right] \\
&\cdot \left\{1 - \frac{43}{160}\lambda^2 + \frac{1}{320}\lambda^4\right\} \quad (\text{A.25})
\end{aligned}$$

and

$$\begin{aligned}
F_{\text{cc}, \pm 1, \text{pro}}^{0p_{jm}, 1s_{1/2m'}}(Q^2) &= \frac{\hbar c}{Mc^2b} \exp\left\{-\frac{19}{78}\lambda^2\right\} \frac{i}{\sqrt{6}} \frac{40}{\sqrt{1365}} \\
&\cdot \left[\delta_{j'3/2} \left\{\delta_{m' \pm 3/2} \delta_{m \pm 1/2} + \delta_{m' \pm 1/2} \delta_{m \mp 1/2} \frac{1}{\sqrt{3}}\right\}\right. \\
&\left. \mp \delta_{j'3/2} \delta_{m' \pm 1/2} \delta_{m \mp 1/2} \sqrt{\frac{2}{3}}\right] \\
&\cdot \left[\frac{1}{2}\Phi_{40}^{\text{cc}}(\lambda) - f_\tau^{\text{cc}}(Q^2) \left\{1 + \frac{39}{160}\lambda^2 - \frac{1}{320}\lambda^4\right\}\right]. \quad (\text{A.26})
\end{aligned}$$

Again we observe the occurrence of an “elastic term” removing the spurious admixtures for the charge and convection current form factors.

Left to be considered are the $2\hbar\omega$ transitions between the $1s$ and the $0s$ hole states in ^{40}Ca . Here, we obtain without projection

$$F_{\text{ch, nor}}^{0s_{1/2m}, 1s_{1/2m'}}(Q^2) = -\delta_{m' m} \exp\left\{-\frac{19}{78}\lambda^2\right\} f_\tau(Q^2) \frac{\lambda^2}{2\sqrt{6}}, \quad (\text{A.27})$$

and

$$F_{\text{sc}, \pm 1, \text{ nor}}^{0s_{1/2m}, 1s_{1/2m'}}(Q^2) = \delta_{m' \pm 1/2} \delta_{m \mp 1/2} \cdot \exp\left\{-\frac{19}{78}\lambda^2\right\} \frac{G_M^\tau(Q^2)\hbar c}{Mc^2b} \frac{\lambda^3}{4\sqrt{3}}, \quad (\text{A.28})$$

while in the COM rest frame, we have

$$F_{\text{ch, pro}}^{0\bar{s}_{1/2m}, 1s_{1/2m'}}(Q^2) = \delta_{m' m} \exp\left\{-\frac{19}{78}\lambda^2\right\} \frac{80}{117} \sqrt{\frac{5}{47}} \lambda^2 \cdot \left[\frac{1}{80} \Phi_{40}(\lambda) - f_\tau(Q^2) \left\{ 1 - \frac{41}{3200}\lambda^2 + \frac{1}{12800}\lambda^4 \right\} \right] \quad (\text{A.29})$$

and

$$F_{\text{sc}, \pm 1, \text{ pro}}^{0\bar{s}_{1/2m}, 1s_{1/2m'}}(Q^2) = \delta_{m' \pm 1/2} \delta_{m \mp 1/2} \cdot \exp\left\{-\frac{19}{78}\lambda^2\right\} \frac{G_M^\tau(Q^2)\hbar c}{Mc^2b} \frac{40}{117} \sqrt{\frac{10}{47}} \lambda^3 \cdot \left\{ 1 - \frac{41}{3200}\lambda^2 + \frac{1}{12800}\lambda^4 \right\}, \quad (\text{A.30})$$

respectively.

References

1. K.W. Schmid, part I, Eur. Phys. J. A **12**, 29 (2001) and references therein.
2. A.E.L. Dieperink, T. de Forest, Phys. Rev. C **10**, 543 (1974).
3. L.J. Tassie, C.F. Barker, Phys. Rev. **111**, 940 (1958).
4. K.W. Schmid, F. Grümmer, Z. Phys. A **337**, 267 (1990).
5. K.W. Schmid, P.-G. Reinhard, Nucl. Phys. A **530**, 283 (1991).
6. T. DeForest, J.D. Walecka, Adv. Phys. **15**, 1 (1966).
7. J.D. Bjorken, S.D. Drell, *Relativistic Quantum Mechanics* (McGraw-Hill, New York, 1964).
8. M.A. Preston, R.K. Bhaduri, *Structure of the Nucleus* (Addison-Wesley, Reading, 1975).
9. T.W. Donnelly, W.C. Haxton, At. Data Nucl. Data Tables **23**, 103 (1979); **25**, 1 (1980).